



## AN ABSTRACT OF THE THESIS OF

Ricardo Orozco for the degree of Master of Science in Electrical and Computer Engineering presented on November 3, 2011.

Title: Optimal Communications System Design for Array-Based Electric Generation

Abstract approved: \_\_\_\_\_

Mario Edgardo Magaña

The world's demand for energy is an ongoing challenge, which has yet to be overcome. The efforts to find clean energy alternatives to fossil fuels have been hampered by the lack of investment in technology and research. Among these clean energy alternatives are ocean waves and wind. Wind power is generated through the use of wind generators that harness the wind's kinetic energy; it has gained worldwide popularity as a large-scale energy source, but only provides less than one percent of global energy consumption. Due to infrastructure limitations on installations of wind turbines at locations where high winds exist, wind energy faces critical challenges difficult to overcome to continue improving electricity generation. Ocean wave energy on the other hand seems like a promising adjunction to wind energy. Ocean energy comes in a variety of forms such as marine currents, tidal currents, geothermal vents and waves. Most of today's research however is based on wave energy. It has been estimated that approximately 257 Terawatt hour per year (TWh/year) could be extracted from ocean waves alone. This amount of energy could be enough to meet the U.S. energy demands of 28 TWh/year. Technologies such as point absorbers, attenuators and overtopping devices are examples of wave energy converters. Point absorbers use a floating structure with components that move relative to each other due to the wave action. The relative motion is used to drive electromechanical or hydraulic energy converters. The total energy throughput of a single point absorber however, does not justify for the great engineering cost and effort

by researchers. Thus the need to explore other alternatives of wave conversion that result in no extra-added cost but yet increases throughput.

Our research focuses on exploring a novel method to maximize wave energy conversion of an array-based point absorber wave farm. Unlike previous research, our method incorporates a predictive control algorithm to aid the wave farm with the prediction of dynamics and optimal control trajectory over a finite time and space horizon of ocean waves. By using a predictive control algorithm, wave energy conversion throughput can be increased as opposed to a system without. This algorithm requires that the wave characteristics of the incoming wave be provided in advance for appropriate processing.

This thesis focuses on designing an efficient and reliable wireless communications system capable of delivering wave information such as speed, height and direction to each point absorber in the network for further processing by the predictive control algorithm. This process takes place in the presence of harsh environmental conditions where the random shape of waves and moving surface can further affect the communication channel. In this work we focus on the physical layer where the transmission of bits over the wireless medium takes place. Specifically we are interested in reducing the bit error rate with a unique relaying protocol to increase packet transmission reliability. We make use of cooperative diversity and existing protocols to achieve our goal of merit and improve end-to-end system performance.

©Copyright by Ricardo Orozco  
Defense Date November 3, 2011  
All Rights Reserved

Optimal Communications System Design for Array-Based Electric Generation

by  
Ricardo Orozco

A THESIS

submitted to

Oregon State University

in partial fulfillment of  
the requirements for the  
degree of

Master of Science

Presented November 3, 2011  
Commencement June 2012

Master of Science thesis of Ricardo Orozco presented on November 3, 2011

APPROVED:

---

Major Professor, representing Electrical and Computer Engineering

---

Director of the School of Electrical Engineering and Computer Science

---

Dean of the Graduate School

I understand that my thesis will become part of the permanent collection of Oregon State University libraries. My signature below authorizes release of my thesis to any reader upon request.

---

Ricardo Orozco, Author

## ACKNOWLEDGEMENTS

Special thank you to Dr. Mario Edgardo Magaña for all his support during my graduate years at OSU. I also would like to thank Roxana Corona for all her love and unconditional support during difficult times. Lastly, I want to thank all of my friends, especially Asher Simons for his friendship and constructive conversations that helped me complete my research.

## TABLE OF CONTENTS

	<u>Page</u>
1 Introduction.....	1
1.1 Overview .....	1
1.2 motivation.....	1
1.3 relevant research.....	4
1.3.1 Ocean Surface Based-Sensor Networks.....	4
1.3.2 Other Wireless Communications On Ocean Surfaces .....	5
2 Background .....	9
2.1 Ocean Waves .....	9
2.2 Wave Shadowing.....	9
2.3 Wave State.....	10
2.4 Wave Energy .....	10
3 Network Description.....	12
4 Physical Layer Description.....	14
4.1 Chanel Characterization .....	14
4.2 Bit Error Rate Performance .....	16
4.2.1 Equivalent Discrete Low-Pass Channel Model.....	16
4.2.2 Spatial Diversity Implementation.....	18
4.2.3 Channel State Information.....	20
4.3 Relaying Protocols.....	20
4.3.1 Amplify And Forward (Aaf) .....	21
4.3.2 Decode And Forward Transmission (Daf) .....	22
4.4 Combining Techniques.....	22
4.4.1 Equal Ratio Combining .....	23
4.4.2 Snr Combining.....	23
4.4.3 Snr Estimation Using Daf.....	23
4.5 Maximal-Ratio-Received Combining .....	24
5 Protocol Design .....	26



## Table Of Contents (Continued)

	<u>Page</u>
5.1 INFORMATION DESCRIPTION .....	26
5.2 Wireless Network Description .....	26
5.3 Payload .....	27
5.4 Wave State Information Flow .....	29
5.5 Transmission Sequence And Channel Partitioning .....	30
5.6 Transmit-Relay Process .....	31
5.7 Time Slot Duration .....	33
5.8 Communication Types.....	33
5.8.1 Network Health Status.....	33
5.8.2 Grid Load Requests .....	35
5.8.3 Wave Farm Expandability .....	35
5.9 Packet Header .....	36
5.10 Relaying Protocol Performance.....	37
6 Simulation Results .....	38
6.1 Parameters .....	38
6.2 Symmetrical Relay Network Used .....	38
6.2.1 Combining Techniques With Aaf - No Csi .....	39
6.2.2 Combining Techniques With Daf - No Csi .....	40
6.2.3 Relaying Comparisons Between AAF And DAF .....	41
6.2.4 AAF Vs. DAF Comparison With Csi.....	42
7 Relay Positioning.....	43
7.1 Relaying Protocol Simulation.....	43
7.1.1 Assumptions .....	43
7.1.2 Packet Loss .....	43
7.1.3 Network Throughput .....	44
7.1.4 Simulation Parameters .....	44
7.2 Special Case Scenarios And Results .....	44

## Table Of Contents (Continued)

	<u>Page</u>
7.3 Relaying Protocol Results .....	50
8 Conclusions And Further Work.....	51
References .....	52

## LIST OF FIGURES

<u>Figure</u>	<u>Page</u>
1.1. Example of a wave energy farm.....	2
1.2. System Architecture.....	5
1.3 Wave shadowing effects on ideal (left) versus realistic (right) waves.....	6
2.1 Shadowing effect produced by WECs.....	9
3.1 Network topology of a wave energy farm.....	13
4.1 Equivalent low pass channel model.....	16
4.2 Multipath and noise effects on signals.....	17
4.3 Diversity technique and DTM .....	18
4.4 Relay positioning with respect to incoming wave.....	19
4.5 Wave Orientation with respect a $(x,y)$ network coordinate system.....	20
4.6 Relayed transmission.....	21
4.7 Receiver combiner.....	24
5.1 On the left a virtual set of rows is implied when an incoming wave.....	29
5.2 Time allocations per frame and time slot.....	30
5.3 Time slot allocation during a transmission process.....	31
5.4 Wave state flow to downstream WECs.....	32
5.5 The <i>poking</i> process.....	33
5.6 Illustrates how the processes are executed with respect to time.....	34
5.7 Multiple transmissions within more than one <i>network instance</i> .....	35
5.8 Packet organizations.....	36
6.1 Amplify and Forward (AAF) with No CSI.....	37
6.2 Diversity with ERC vs. Single link transmission.....	38
6.3 SNR vs. ERC combining using AAF.....	39
6.4 ERC vs. SNRC Comparison.....	40
6.5 AAF compared to DAF.....	41

## LIST OF FIGURES (Continued)

<u>Figure</u>	<u>Page</u>
6.6. DAF vs. AAF with CSI.....	41
7.1 Radio Node Communication Network on a 100 m x 100 m grid.....	44
7.2 Three node network.....	44
7.3 The throughput and BER are shown for a 3-relay network.....	45
7.4 Source with multiple relay options.....	46
7.5 No relay available for source node.....	47
7.6 Scenario where direct transmission is not available.....	48
7.7 Simulation results using one and two retransmissions.....	49

## LIST OF TABLES

<u>Table</u>	<u>Page</u>
1.1 Wave energy availability within the U.S.....	41
1.2 Wave state description .....	26
1.3 Payload .....	27
1.4 Packet Structure .....	28
1.4 Simulation Parameters.....	43

# 1 INTRODUCTION

## 1.1 Overview

In a wireless propagation scenario the signal suffers from poor channel quality due to the fading effects from multipath propagation. For example, low sea level transmissions, as in a wave energy converter (WEC) farm, signals are severely affected by the random sea surface which blocks the line of sight between transmitter and receiver. Therefore, multipath is one of the key factors that prevents predictable and reliable wireless communication between WECs. This work uses a new protocol design to combat the multipath effects caused by ocean wave activity by means of *spatial diversity* achieved by a WEC farm antenna array. The performance of the new protocol is compared to existing ones showing improvement in communication bit error rate and throughput.

## 1.2 Motivation

The lack of clean energy source alternatives has motivated the research into the potential to exploit the available energy in ocean waves. According to the National Renewable Energy Lab (NREL), approximately 257 TWh/yr could be extracted from ocean waves alone. This amount of energy could be enough to meet U.S. demands of 28 TWh/year [16]. Table 1.1 lists the locations of wave resources by region within the U.S.

**Table 1.1 Wave energy availability within the U.S.**

US Wave Resource Regions (>10kW/m)	TWh/yr.
New England and Mid-Atlantic States	100
Northern California, Oregon and Washington	440
Alaska (exclusive of waves from the Bering Sea)	1,250
Hawaii and Midway Islands	330

Unlike wind energy where infrastructure constrains and unpredictable wind patterns hinder continuous energy exploitation, ocean waves are easily accessible and highly predictable year round. The cyclic wave patterns due to winds blowing over

hundreds of kilometers away over large areas make ocean waves an excellent and everlasting clean energy source.

One of the most popular wave energy converters is the point absorber. A point absorber uses a floating structure with components that move relative to each other due to the wave action. This relative motion (up and down) is used to drive the electromechanical or hydraulic energy converters. Although current point absorber designs serve as a proof of concept for wave energy conversion, their energy throughput does not justify for the high design & maintenance costs. Therefore new solutions have been proposed including the concept of an *array-based* point absorber wave farm. Unlike regular wave farms, we present an energy wave farm aided with a predictive control algorithm to further increase electricity generation. The predictive control unit allows each point absorber to match the wave's resonance frequency and thus convert maximum kinetic energy to electricity. Our work focuses on the generic point absorber that moves up and down as a result of waves motion. Without loss of generality, we refer to the generic point absorber as wave energy converter (WEC) throughout this work. An example of a 3 by 3 WEC arrangement in a wave energy farm (WEF) is presented in Figure 1.1. In this figure only the WEC configuration is shown. According to [18,49] when a WEC is aided with a predictive control algorithm, its throughput can increase by a factor of four compared with a wave farm without predictive control.

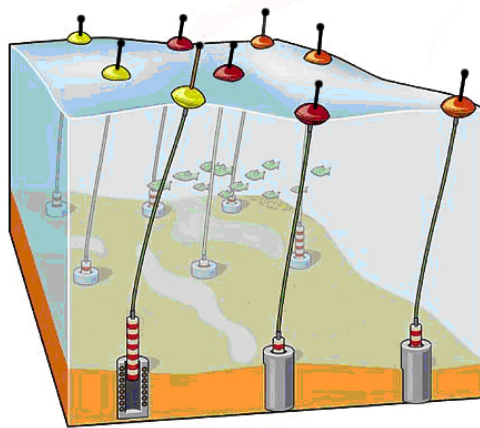


Figure: 1.1 Example of a wave energy farm.

The resources available at Oregon State University such as the L10 energy converter and unlimited high waves off the coast of Oregon make this research especially attractive. In fact, tests have already been conducted on the L10 prototype and the results showed a yearly average power generation of 30 kW/mcl. We hope to further increase this throughput by incorporating the predictive control algorithm. The increase in throughput can be briefly explained through the use of a bicycle ride example. If a person rides a bicycle at constant speed wants to go faster, the person needs to first adjust the pedaling to the bicycle's current speed and only then can the person achieve the desired speed gain. Using this analogy, each WEC can tune itself to incoming wave trajectories, speeds and frequencies to optimize its energy conversion. This approach is different from Today's mechanical WEC designs where only one finite and deterministic frequency response is available.

The contribution that this work exploits is the design of a low power radio communication system capable of communicating wave characteristics like wave velocity, height and phase angle needed by the predictive control algorithm at each WEC in the wave farm. This work demonstrates relevant techniques used to mitigate bit error propagation under harsh environmental conditions near the ocean surface, especially when the line-of-sight (LOS) between the transmitter and receiver is partially blocked due to high waves. Furthermore a relaying protocol is presented to increase the communications system reliability i.e. making sure information packets are delivered on timely manner under harsh conditions. In addition to maintaining wireless network working under normal conditions, the protocol reports the WECs working conditions and wave farm's electricity throughput to off shore base station to further process this information with the GRID.

A reliable network could be achieved in two ways: (1) using physical wires or (2) via a wireless communications system. Connecting network nodes with wires is a simple and practical solution. Cables provide wide bandwidth, security and almost error free communication. However, at sea, cables are expensive and non-portable. In addition, cables maintenance costs can be very expensive and could pose a potential hazard to the marine life. Wireless networks on the other hand, are relatively cheap and portable.



Communication hubs can be placed within the WECs, sharing environment-proof space that is easily accessible for maintenance if needed. With low power transmissions and plenty of power to tap off if needed, a wireless communication system requires minimal maintenance and is relatively cheap. From our analysis, we believe that the wireless system is the best communication method. As a proof of concept we design a communication system on 3 by 3 wave farm. This work however could be potentially expanded to other applications in the field of sensor-based networks, wind farms on oceans or wild fire networks.

The outline of this thesis is as follows: Chapter 1 concludes with a review of previous work done in the field of ocean communications. Chapter 2 goes over essential background information about waves and wave energy. Chapter 3 describes the network presented in this thesis. Chapter 4 describes the communications system. Chapter 5 describes the relaying protocol design and finally chapter 6 draws the conclusions and outlines future work.

## **1.3 Relevant Research**

### **1.3.1 Ocean Surface Based-Sensor Networks**

One of the most contemporary and common applications of sensor networks is in the environmental monitoring field. For example, sensor networks are deployed specifically for taking sea temperatures, monitoring offshore fishery or tracking debris [36]. Many sensor network such as the one presented in [36] are based on the deployment of wireless TelosB modules. These sensors include a standing structure, battery and antenna. These nodes can communicate to a base station, which in turn transmits the collected data to a database server. The work in [36] has some specific similarities to the work presented in this thesis, specifically the way in which data is transmitted to the base station as shown in Figure 1.2.

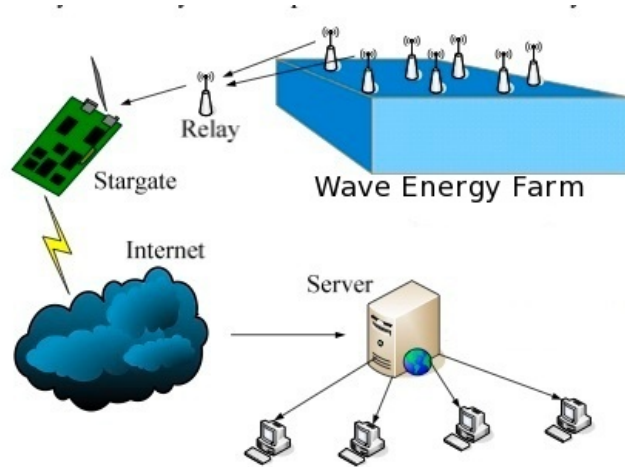


Figure: 1.2 System Architecture.

However there are fundamental differences between our work and [36]. For example, in [36] and unlike our work, sensors require constant maintenance such as battery replacements that add costs. More importantly our work is based on designing our radio communication system, which does not adhere to a specific wireless technology standard. Furthermore the bidirectional node communication is particularly important to the wave farm in order to maintain accurate wave state information for the predictive control algorithm and the GRID off shore. By using our own protocol design, we are able to control the transmitting power and other important components such as antenna type and size that would otherwise result in added cost and inadequate application

### 1.3.2 Other Wireless Communications on Ocean Surfaces

Current maritime communication systems are based on radios for ship-to-shore communications near port waters and satellite communication for long-range ship-to-ship and ship-to-shore communications [43]. Our work is similar to [43] the way in which a link is established between two nodes out of range. In such case, other nodes within range are used to relay the information until the destination is reached. This is mainly the only similarity to our work as the infrastructure is clearly different. For example, each node will have one antenna 1 m in height and positioned on top of the WEC. Communication is especially challenging in rough sea conditions since the line-of-sight

between transmitter and receiver is often times blocked by high waves that cause a weak communication link. From [43] it is shown that two ships must carry a high-gain antenna placed on top of ships in order to improve a communication link. However the large equipment and high gain antennas result in added cost and impractical application to WECs due to size and budget constraints.

A different approach for increasing a line-of-sight on ocean surfaces is described in [55]. Their work is based on deploying a large number of relay nodes so that during each transmission, a neighboring node is always available to forward the information. This process is repeated until the final destination is reached. The total number of nodes in [55] is determined by computing the average wave heights from collected wave information over a given period of time in a specified area. This main idea is illustrated in Figure 1.3 (left). The solution presented in [55] is simple but not practical; adding hardware adds to cost and cannot guarantee packet delivery under harsh environmental conditions. A comparison of a realistic vs. an ideal wave is presented in in Figure 1.3. From the figure it can be seen that a line-of-sight between two points may or may not be feasible due to the random shapes of waves as supposed to the idea presented in [55].

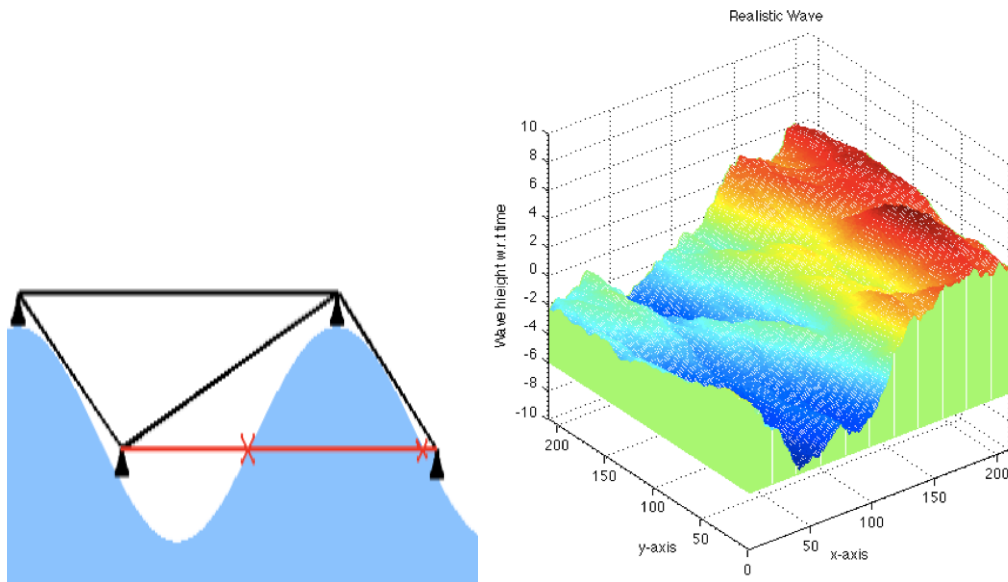


Figure: 1.3 Wave shadowing effects on ideal (left) versus realistic (right) waves.

Other works have also proposed improving intelligent protocols at the LINK layer, capable of retransmitting as need until data packets reach the destination. Among some of these protocols are the destination-sequenced distance-vector (DSDV) [12], zone routing protocol (ZRP) [7] and ad-hoc on-demand distance vector (AODV) [11]. Below we briefly describe each protocol.

The DSDV is a proactive routing protocol that builds a network topology by constructing and maintaining a routing table in each sensor. Routing tables however, consume a lot of processing time, bandwidth and power. Mainly, this protocol is intended for mobile networks with hundreds of nodes. Furthermore, due to the multi-hop transmissions, nodes tend to be equipped with large memory space to handle this extra load. However unlike [12], our work focuses on efficiency and one-hope transmissions without the use complex protocols.

The AODV is a reactive protocol whose algorithm is only triggered when a node has a request [11]. Its main goal is to select the shortest path from sender to receiver in mobile networks. Although this protocol solves many flaws from DSDV, the degree of complexity also increases and does not benefit static networks, especially when the surface is constantly changing. In addition, the discovery process from [11] adds more processing time and increases power consumption. Similarly as above, these drawbacks are precisely what we intend to avoid.

The ZRP protocol offers an alternative to both AODV and DSDV. This protocol is based on the idea of adjustable routing zones by increasing or decreasing the transmitting power [7]. This eliminates the need to maintain large routing tables and excessive waste of resources such as memory. One drawback of this protocol occurs when the line-of-sight between source and destination is lost, causing an unlimited number of retransmissions. These scenarios are likely to occur during rough sea state conditions where high waves are predominant and whose potential energy content is great. Consequently the changing sea surface hinders the advantages of this protocol.

An entire different approach proposed by [4] to conduct sea surface network communication is through underwater transmissions. The goal is to avoid the problems presented by high waves and weak communication links. While acoustic communication

has high range underwater, it has high and variable propagation time, high bit error rate, and high-energy consumption.

Any of the wireless communication methods mentioned above could potentially be used to transfer information within the wave farm, but would result in an inefficient wireless network. Therefore, in this thesis, we design a unique and practical communication system that meets the specific requests of the network presented in this work. The design is based on existing features from the protocols described above as well as new enhancements suitable for static networks. Our goal is to establish a reliable communication link between a source and destination nodes presented under harsh sea conditions.

## 2 BACKGROUND

### 2.1 Ocean Waves

High-energy waves are caused by the wind blowing over large surface areas for long distances. The constant wind patterns (such as the trade winds or westerlies) and storms allow researchers to locate zones of high-energy concentration to conduct further research on the topic. These waves that originate hundreds of kilometers away can travel long distances with little energy loss, which means that energy conversion is possible even in places where no wind patterns are present. In brief, wave energy is transformed from kinetic and potential forms to electricity via wave energy converters whose components move relative to each other due to the wave action to drive electromechanical or hydraulic energy converters [54].

### 2.2 Wave Shadowing

When a wave passes a WEC, a natural wave-shadowing phenomenon is created. This is the zone of lower energy concentration due to the obstruction of the wave as it passes the WEC. The shadowing zone has a greater effect on energy concentration closer to the obstructing WEC, but diminishes with distance. Figure 2.1 shows a simple drawing of the shadowing effect [14,46,49].

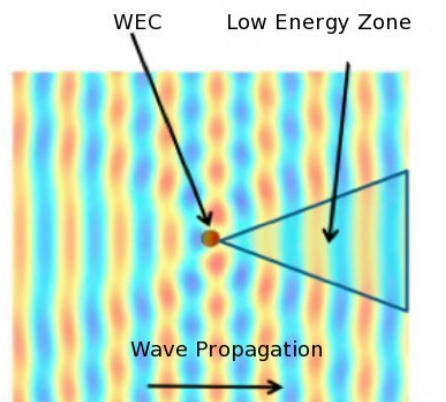


Figure: 2.1 Shadowing effect produced by WECs.

The zones of low energy concentration are typically and therefore in this work we assume each WEC is placed far apart from each other (100 m) and consequently the waves reach a different sea state and energy content when they reach another WEC. Hence, the operation of one WEC does not impact the operation of another. This is a common assumption for wave farm analysis as the combined shadowing effects are not yet well understood [15,18,31].

## 2.3 Wave State

The total wave energy concentration is dependent of its height, speed and phase angle. In this work we refer to these wave attributes as *wave state*. So WECs will receive *wave state* information via the wireless communication network. The information will then be processed to the predictive control algorithm and used by the WEC to adjust local control settings to optimize energy conversion.

## 2.4 Wave Energy

In brief, the energy in a wave is the amount of energy it takes to move water particles from point A to point B. T. Brekken [10] explains in detail how ocean wave energy is converted to electricity energy. His work is briefly summarized here.

The energy in water travels at group velocity  $v_g$ , which is the velocity at which groups of waves move. This group velocity can be described as a function of wavelength and is directly related to the total power in a wave. More specifically, the power in a wave can be computed from calculating the energy per longitudinal unit of length. Multiplying the energy per length and energy transmission velocity yields the power delivered, namely

$$P = J_\lambda \cdot v_g. \quad (2.1)$$

The energy per wavelength  $J_\lambda$  becomes the total energy required to move every water particle from the trough to the crest of a wave. This results in the total potential energy per unit of crest length. By using the equipartition of energy,  $J_\lambda$  is related to the potential energy, which is equal to the kinetic energy, namely

$$J_{\lambda} = \frac{1}{2} \rho g a^2 [J / m], \quad (2.2)$$

where  $\rho$  is the water density of approximately  $1025 \text{ kg/m}^3$ ,  $a$  is the wave amplitude and  $g$  is the acceleration due to the earth's gravity of  $9.81 \text{ m/s}^2$ . The power per meter crest length (mcl) per wave becomes

$$P = \frac{1}{4} \rho g a^2 \sqrt{\frac{g \lambda}{2\pi}}, \quad (2.3)$$

where  $\lambda = v_p \cdot T$ ,

the phase velocity  $v_p = \sqrt{\frac{g \cdot \lambda}{2\pi}}$  and  $\lambda$  is the wavelength. Therefore,

$$P = \frac{1}{4} \frac{\rho g a^2 T}{2\pi} = \frac{\rho g^2 H T}{32\pi} [P / m], \quad (2.4)$$

where  $H$  is historically defined as wave height from trough to crest and is equal to  $2a$  and  $T$  is the wave period.

From equations (2.3) and (2.4) it can be seen that power,  $P$ , is proportional to the wave height squared and the square root of the wavelength and linearly proportional to the wave period. The results obtained by Brekken also match those discussed by Falnes and McCormick in [18, 34] respectively. The reader is encouraged look at these sources for further details. Next we describe how the wave farm is structured and how we plan to deploy the wireless communication system.



### 3 NETWORK DESCRIPTION

For the purposes of this study, the network is comprised of nine WECs, placed 100 meters apart from each other along the  $x$  and  $y$  axis on a  $x$ - $y$  grid. Each WEC is assumed to be equipped with a communication node and one transmitting antenna. The nodes are able to transmit or receive information from neighboring nodes but cannot perform both at the same time. In addition to the nine WECs in the wave farm, four *wave riders* are also incorporated to the network. These *wave riders* are a class of buoys that are used for data collection purposes only and whose design are lightweight to ‘ride the wave’, allowing wave data to be collected without being corrupted by the buoy motion. In this work we assume the *wave riders* are able to determine full wave state (i.e. wave height, direction, phase angle and speed) but the details on how this is done shall be determined in future work. A top view of a mesh topology we believe will yield good results is shown in Figure 3.1. Each node is uniquely identified by a node ID and can communicate with its immediate neighbors. Any transmissions by nodes out of range are treated as noise. Furthermore, all WECs are assumed to be moored to the ocean as shown in Figure 3.1. The total number of nodes and wave riders presented in this work is only for proof of concept and does not impose a limit on the network size; commercial-scale wave farms, for example, will likely contain hundreds of WECs.

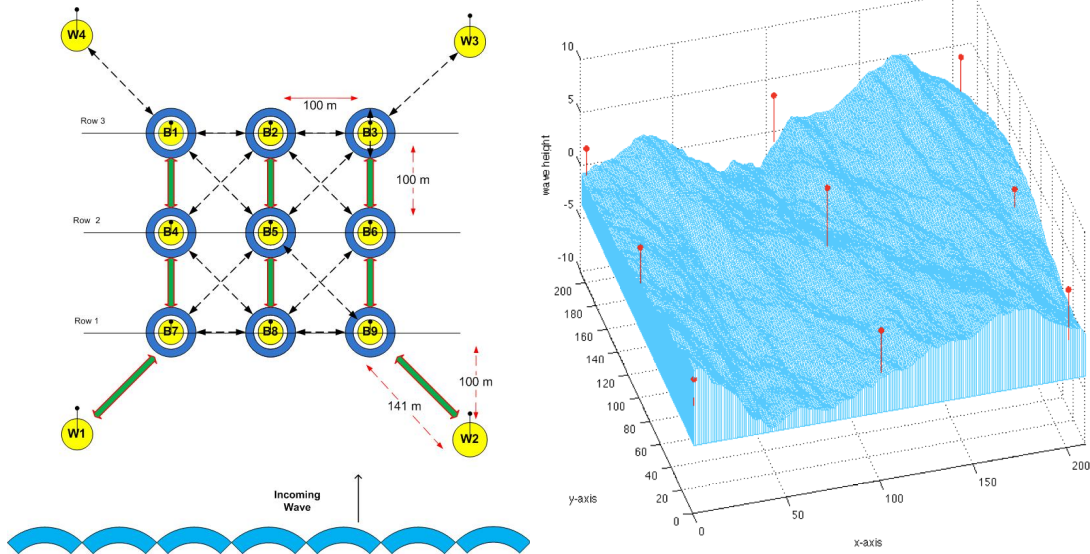


Figure: 3.1 Network topology of a wave energy farm. Node identification codes are B# and W# for buoy or wave rider respectively. On the right, a realistic ocean surface of 100 m by 100 m was generated using experimental data.

## 4 PHYSICAL LAYER DESCRIPTION

The first thing we consider is the channel characterization at the physical layer. With sufficient understanding of the communication channel, the bit error rate (BER) can then be calculated and analyzed to select a good signal-to-noise-ratio (SNR) that achieves the desired BER performance.

### 4.1 Chanel Characterization

In maritime communication systems, multipath fading due to sea surface reflections generates signal degradation at low elevation angles. Furthermore, the link quality between two nodes deteriorates when their line-of-sight is blocked by high waves. Previous work done by researchers in this field have conducted real-life experiments under similar conditions and collected enough data to characterize the fading channel [28,41,42,43]. Next we highlight two of these approaches in order to understand some of the challenges in maritime communications.

Maritime radio communication at low elevation angles is affected by the rough sea surface profile [28,41,42,43]. This is in part due because the sum of the coherent and incoherent components plus the direct line of sight at the receiver. Specifically, Karasawa [30] showed that there exists a direct relationship between power fading and wave heights. His work is based on the Kirchhoff approximation theory where the effects of shadowing and sea surface conditions are taken into account. These theoretical results are also compared to experimental data collected based on received average power. From [30]'s conclusions, it was discovered that under rough sea state conditions (i.e. waves of up to six meters in height) the received noncoherent power dominates over coherent.

A different approach was taken by An in [5]. Rather than taking direct experimental power measurements, which requires a large computation, data load, [5] derives a statistical model for the mean incoherent power based on gross propagation path-loss. An compared his results to [30] for accuracy and consistency. Below is a brief summary of his work.

The incoherent component of a reflected signal from the sea surface is random in phase and amplitude due to the random facets on the wave. There are two major components directly related to signal integrity. First is the *sea roughness*, which is a coefficient that is proportional to the phase difference between the coherent and incoherent signal reflections [30]. This is described by

$$\beta_i = 4 \cdot \frac{\pi}{\lambda} \cdot H_m \cdot \sin(\theta_i), \quad (4.1)$$

where  $\lambda$  is the signal's wavelength,  $\theta_i$  is the elevation angle,  $H_m$  is the wave height from trough to crest and  $N$  is the total number reflected signals. Realistically, it is impractical to analyze all possible signal reflections of a signal on a sea surface as pointed out by [5] and instead a new approach proposed. It was proved in [22,31] that the reflection coefficients of a sea surface can be modeled as a complex random variable  $\alpha_i$ , especially under rough sea state conditions. These findings were later used by [5] to derive a statistical approach rather than experimental to characterize the channel. Mainly [5] describes the received total signal as

$$E_r = E_0 \left\{ 1 + \sum_{i=1}^N \alpha_i \cdot \exp[j \cdot \beta_i] \right\} \quad (4.2)$$

where  $E_0$  and  $\alpha_0=1$  is the field strength of direct path and its reflection coefficient respectively,  $E_r$  is the total energy received,  $\beta_i$  is the roughness of the reflection components (relative to each coherent reflection component) and  $N$  is the total number of reflections. From (4.2) it was noted that  $E_r$  approaches the Rician distribution when a direct path exists [5]. However, a Rayleigh distribution becomes apparent when  $\beta_i > 2$  because the incoherent components is dominant. By performing experiments on waves of 3 meters or higher, [5] proved that there exists a linear relationship with power fading and sea wave height. From his results it was clear that the reflection power for higher waves have higher fading intensity and as opposed to smaller waves. From the results obtained, it was found that for waves less than 2 m in height, the CDF for the received average power follows a Rician distribution whereas for waves greater than 3 m it

follows the Rayleigh distribution. In this work we model the fading channel based on the Rayleigh distribution.

## 4.2 Bit Error Rate Performance

Next we describe some of the factors affecting reliability in a communication system. Specifically, this section describes how diversity is used to mitigate multipath effects.

### 4.2.1 Equivalent Discrete Low-Pass Channel Model

Radio signals propagate through the medium and undergo random changes in both amplitude and phase. An equivalent low-pass communication channel is shown in Figure 4.1 used in our simulations. Both path-loss and multipath are multiplicative while the thermal white noise is additive. For our work we use binary phase shift keying (BPSK) to modulate signals from source to destination.

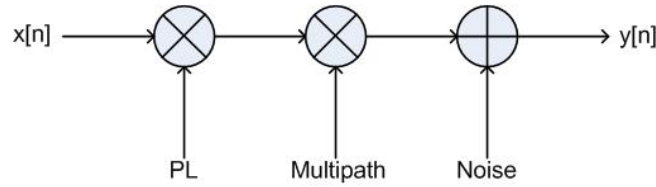


Figure: 4.1 Equivalent low pass channel model.

The multiple signal reflections from the sea surface with different phases and amplitudes add destructively at the receiver. Since the number of signal reflections is relatively “large”, the central limit theorem can be applied to model the received signal as a random process [19,29]. Furthermore, the noise introduced by the RF components and amplifiers at the receiver can be characterized statistically as an additive complex Gaussian process [19]. Since the equivalent discrete system is a representation of a narrow band-pass noise, noise is represented as the sum of the real and imaginary parts. These are statistically independent, each having a zero mean and variance  $\sigma^2 = N_0/2$ , yielding a total noise power of  $N_0 = 2\sigma^2$ . Thus, the received signal can be described as

$$y_d = d_{s,d} \cdot a_{s,d} \cdot x_s + z_{s,d} = h_{s,d} + z_{s,d}, \quad (4.3)$$

where  $d_{s,d}$  and  $a_{s,d}$  are the path loss and multipath respectively. Both of these effects are also represented by  $h_{s,d}$  whereas noise is represented by  $z_{s,d}$ . The fading effects are shown in Figure 4.2. Multipath is critical in a communication system since it is one of the main contributors to erroneous bit detection at the receiver. One solution to the fading problems is achieved by increasing the transmitting power as show in the figure.

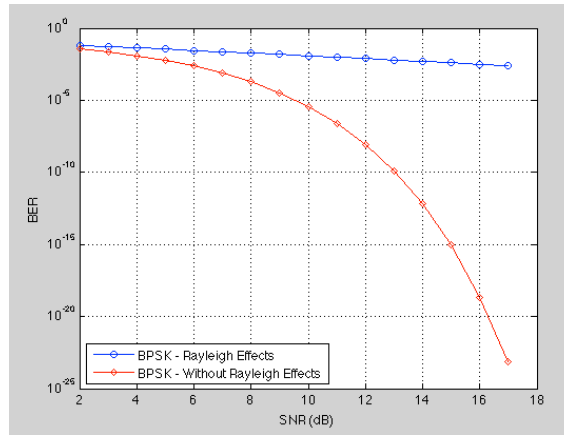


Figure: 4.2 Multipath and noise effects on signals.

Another technique to mitigate multipath effects is via *diversity* technique [2]. In his work, [2] shows that two transmitting and one receiving antennas provides the same diversity as the maximal-ratio receiver combining (MRRC) with one transmit antenna, and two receive antennas. But, implementing either technique poses a challenge because of each WEC would require more than one antenna. Therefore an alternative solution is to create a virtual antenna by sharing the antennas from other WECs.

### 4.2.2 Spatial Diversity Implementation

Spatial diversity refers to the technique where one or more relay nodes are used to cooperate in the transmission between source and destination. At the receiver, the received replicas appear to be coming from a single multi-array source, thus the term of a *virtual antenna array*. Consider the three-node model shown in Figure 4.3 (left). In addition in order to maintain a practical system, we only consider one communication channel. Consequently, we employ a *Time Domain Multiplexing* (TDM) technique to avoid interference among the nodes. This technique consists in allocating specific time slots or *sub channels* to each node to transmit as shown in Figure 4.3 (right). The process is repeated after the last node's turn is over. From the three-node model configuration presented in the figure, the source transmits to the relay and destination during the first time slot. The relay then retransmits the information received to the destination during the second time slot. From the figure  $h_{(i,j)}$  represents the channel fading coefficients in the various directions and s,r,d are the source, relay, and destination respectively. The  $T_{x(s,(r,d))}$   $T_{x(r,s)}$  depicts sub channels from source to relay-destination and relay-source respectively.

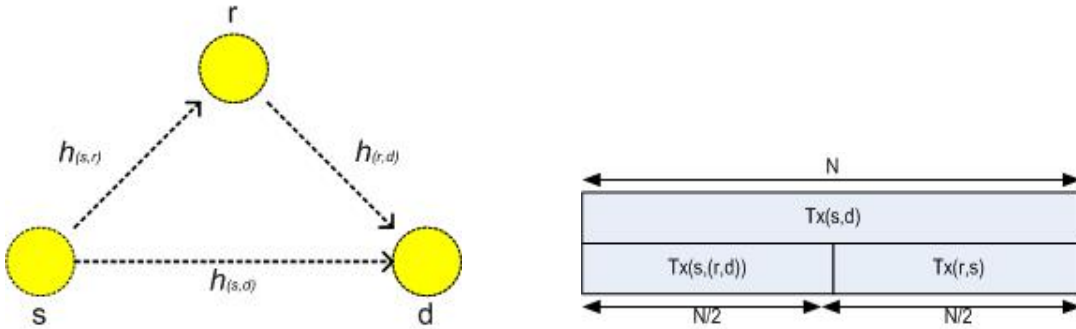


Figure: 4.3 Diversity technique (left) and TDM (right) used to avoid channel interference.

It has been shown that spatial diversity achieves the same performance as having two-transmitting and one receiving physical antennas [2]. The performance is due to the multiple signal replicas received from the source and relay(s). From [2] when the antennas (i.e. relays) are placed *far apart* from each other, signals undergo different fading both in phase and amplitude. This decreases the probability that all signals

undergo the same fading and increases the chances at the receiver to detect the correct symbols [2,19,29]. In this work we take advantage of the spatial diversity benefits to reduce BER at the expense of reduced bandwidth.

Depending on the ocean's currents, waves may impact at the wave farm from various directions. Two of the foremost important cases considered in this work are shown in Figure 4.4. The WECs are shown in yellow and the communication nodes in black. From the figure, a wave approaches node B1 that then has to send wave state information to B4 and B5 respectively. Therefore to reduce BER we make use of the available relays B1 and B4 (left) and B2 and B5 (right) respectively.

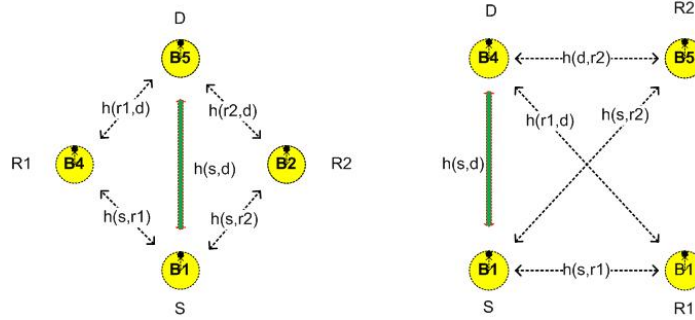


Figure: 4.4 Relay positioning with respect to incoming wave.

Another possible case is shown in Figure 4.5, where the angle describes the incidence angles of wave approaching the wave farm. From the figure shown, the incoming wave has an incidence phase angle of twenty-degrees.



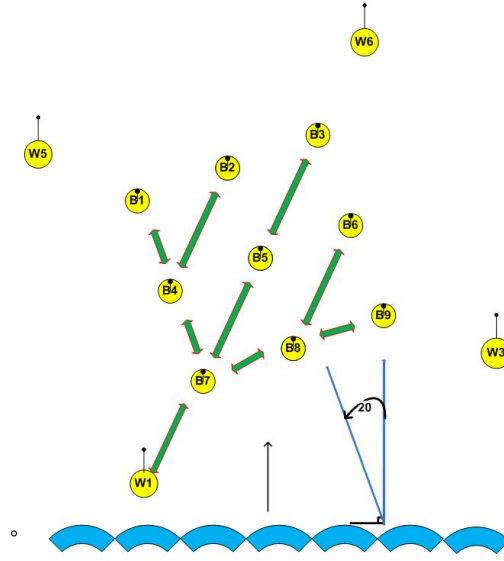


Figure: 4.5 Wave Orientation with respect a  $(x,y)$  network coordinate system.

### 4.2.3 Channel State Information

One important aspect of spatial diversity is *channel state information* (CSI). The CSI is used to describe the total power attenuation experienced by signals due to path-loss and multipath. In cases where signals suffer from a known constant fading, a simple solution is to increasing the transmitting power. However in most cases, this is not the case and signals undergo some random fading (both in phase and amplitude) not easily detectable by the receiver. The fading is described by the CSI coefficients  $h(i,j)$  as shown in Figure 4.4. For highly accurate wireless communication systems, a dedicated pilot signal is used to determine CSI before sending information packets; this helps in making more accurate detection decisions at the receiver [3,32]. Therefore for our simulations, we assume the receiver has full channel state knowledge represented by the  $h(i,j)$  coefficients, where  $i,j$  indicate the origin and destination respectively.

### 4.3 Relaying protocols

Laneman in [32] outline low-complexity protocols used for cooperative using the TDM technique described in the previous section. Two of the most popular are amplify and forward (AAF) and decode and forward (DAF). In our work we compare both

protocols via computer simulations as well as different combining techniques at the receiver. From the results obtained, we select the best protocol and combining technique that achieves the best BER performance.

### 4.3.1 Amplify and Forward (AAF)

This protocol forwards the received noisy signal  $y_r$  at the relay to the destination after amplifying it by some  $\beta$  factor as shown in Figure 4.6. The amplification  $\beta$  factor is determined based on the transmitted power  $P$  from the original source [3,21].

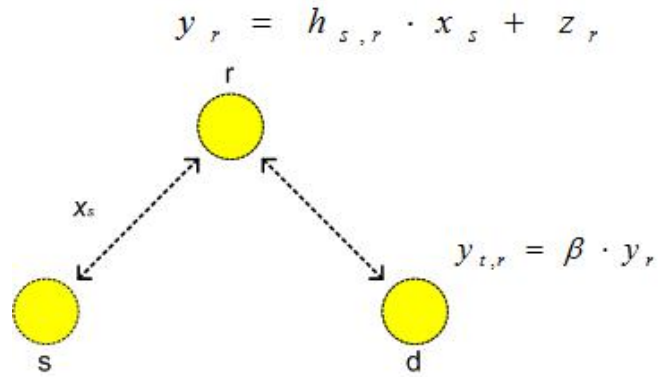


Figure: 4.6 Relayed transmission.

The signal  $y_r = h_{s,r} \cdot x_s + z_r$  is the received signal at the relay with fading coefficient  $h_{s,r}$  and noise  $z_r$ . After amplifying the signal by some  $\beta$  factor, it is then transmitted to the destination and becoming  $y_{t,r} = \beta \cdot y_r = \beta \cdot (h_{s,r} \cdot x_s + z_r) + z_d$  or equivalently  $y_d = \beta \cdot (h_{s,r} \cdot x_s + z_r) + z_d$ . Then the autocorrelation of the received signal  $y_d$  becomes

$$y_d = \beta \cdot (h_{s,r} \cdot x_s + z_r) + z_d \quad (4.4)$$

$$\begin{aligned} E\{|y_d|^2\} &= E\{y_d \cdot y_d^*\} \\ &= E\left\{\left(h_{r,d} \cdot \beta \cdot (h_{s,r} \cdot x_s + z_r) + z_d\right)\left(h_{r,d} \cdot \beta \cdot (h_{s,r} \cdot x_s + z_r) + z_d\right)^*\right\} \end{aligned} \quad (4.5)$$

where,

$$E\{z_d\} = E\{z_r\} = 0, \quad (4.6)$$

$$E\{|z_d|^2\} = E\{|z_r|^2\} = N_0 = N_0 \quad (4.7)$$

$$E\{z_d \cdot z_r^*\} = 0 \quad (4.8)$$

$$E\{z_d \cdot x_s^*\} = 0 \quad (4.9)$$

Expanding on equation (4.5),

$$\begin{aligned} &= E\left\{\left(h_{r,d} \cdot \beta \cdot (h_{s,r} \cdot x_s + z_r) + z_d\right)\left(h_{r,d} \cdot \beta \cdot (h_{s,r} \cdot x_s + z_r)^* + z_d^*\right)\right\} \quad (4.10) \\ &= E\left\{\left(h_{r,d} \cdot h_{r,d}^* \cdot \beta^2 \cdot (h_{s,r} \cdot x_s + z_r)(h_{s,r} \cdot x_s + z_r)^* + h_{r,d} \cdot z_d^* \cdot \beta \cdot (h_{s,r} \cdot x_s + z_r) + z_d \cdot h_{r,d} \cdot \beta \cdot (h_{s,r} \cdot x_s + z_r)^* + z_d \cdot z_d^*\right)\right\} \\ &= E\left\{h_{r,d} \cdot h_{r,d}^*\right\} \cdot \beta^2 \cdot E\left\{(h_{s,r} \cdot x_s + z_r)(h_{s,r} \cdot x_s + z_r)^*\right\} + \\ &\quad E\left\{h_{r,d} \cdot \beta \cdot (h_{s,r} \cdot x_s + z_r)\right\} E\{z_d^*\} + E\left\{z_d \cdot h_{r,d} \cdot \beta \cdot (h_{s,r} \cdot x_s + z_r)^*\right\} + \\ &\quad E\{z_d \cdot z_d^*\} \\ &= \beta^2 \cdot E\left\{h_{r,d} \cdot h_{r,d}^*\right\} \cdot E\left\{h_{s,r} \cdot h_{s,r}^* \cdot x_s \cdot x_s^* + h_{s,r} \cdot x_s \cdot z_r^* + z_r \cdot h_{s,r}^* \cdot x_s^* + z_r \cdot z_r^*\right\} + N_0 \\ &= \beta^2 \cdot |h_{r,d}|^2 \cdot (|h_{s,r}|^2 \cdot \xi_s + N_0) + N_0 \end{aligned} \quad (4.11)$$

where  $E\{|y_d|^2\} \leq P$ , yielding

$$\beta^2 \cdot |h_{r,d}|^2 \cdot (|h_{s,r}|^2 \cdot \xi_s + N_0) + N_0 \leq P \quad (4.12)$$

### 4.3.2 Decode and forward Transmission (DAF)

This protocol decodes the received noisy signal  $y_r$  at the relay and retransmits the newly encoded signal to the destination with the same transmitting power as the source. In order to avoid bit error propagation, we only forward correct information packets to the destination. If errors are detected, the packets are dropped.

## 4.4 Combining Techniques

In this section we describe some techniques used at the destination to combine the different and independent fading signals. The decision device then makes the final

determination to what signal was received. Some of these techniques vary in complexity leading to better performance.

#### 4.4.1 Equal Ratio Combining

Equal Ratio Combining (ERC) technique is simple and practical but performance is not as good compared to other techniques. The receiver combines the incoming signals after the co-phasing process (i.e. the process at the receiver used to identify phase shifts on incoming signals). The received signal at the destination from the source and destination is given by

$$y_d = \sum_{i=1}^k h_{i,d}^* \cdot y_{i,d} \quad (4.13)$$

#### 4.4.2 SNR Combining

This technique weights the received signals with their respective received SNR values. The signals are then combined and passed to a decision device to determine the output at the destination. From (4.12) and  $\beta = 1$ , the received SNR becomes

$$SNR = \frac{|h_{r,d}|^2 \cdot |h_{s,r}|^2 \cdot \xi_s}{|h_{r,d}|^2 \cdot \sigma_{s,r}^2 + \sigma_{r,d}^2} \quad (4.14)$$

#### 4.4.3 SNR Estimation using DAF

The received SNR can be determined by analyzing the bit error rate. The theoretical BER for BPSK under Rayleigh fading conditions is given by

$$BER = 0.5 \left( 1 - \sqrt{\frac{\bar{\gamma}}{1 + \bar{\gamma}}} \right) \quad (4.15)$$

where,  $\bar{\gamma} = \frac{\epsilon_b}{N_0} E[\alpha^2]$

and  $E[\alpha^2]$  is the average value of  $\alpha^2$ . Thus solving for  $\bar{\gamma}$  in (4.15) yields a SNR value equal to

$$SNR = \frac{1}{2} [Q^{-1}(BER)]^2 \quad (4.16)$$

Therefore the total BER becomes

$$BER_{s,r,d} = BER_{s,r} \cdot (1 - BER_{r,d}) + (1 - BER_{s,r}) \cdot BER_{r,d} \quad (4.17)$$

## 4.5 Maximal-Ratio-Received Combining

With maximal-ratio-received combining (MRRC) each signal is multiplied by the conjugate of its estimated fading channel coefficient gain and then combined as shown in Figure 4.7. The estimated received signal for a 3-node configuration shown in Figure 4.6 becomes

$$\tilde{X} = h_{s,d}^* y_{s,d} + h_{r,d}^* y_{r,d} \quad (4.18)$$

where  $s, r, d$  are source, relay and destination respectively.

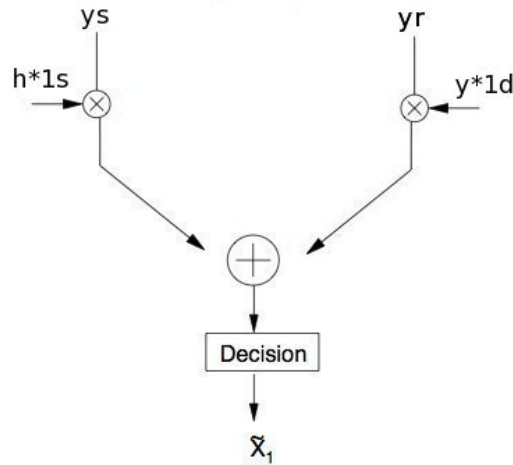


Figure: 4.7 Receiver combiner

## 5 PROTOCOL DESIGN

In this chapter we propose a reliable relaying protocol capable of delivering information packets safely under the harsh environmental conditions presented near the sea surface. The specific design we propose uses some of the concepts from [7,11,12] as well as new features to assure reliability. Next we describe the types of information relayed by nodes in the network.

### 5.1 Information Description

The first type of information being transmitted among the nodes is the wave state information. Furthermore, it is important to continuously check the working conditions or *health* of the different components in the wave farm such as the WECs or the communication nodes. Lastly the need to communicate periodic loads inquired by GRID to the wave farm is also important so that no electricity is lost due to mismatches. Wave state information is used for the predictive control algorithm to auto-tune downstream WECs to incoming waves and maximize energy conversion. The second type helps maintain a fully functional wave farm by ensuring each WEC and node work under normal operational condition. The information is then forwarded to a base station offshore to alert the farm operators and take further action if needed. Finally GRID electricity demands may change from time to time so it is important to relay this information to the wave farm and synchronize each WEC.

The information data packets are of relatively small (i.e. a few bytes) but sufficiently large to coordinate wave farm functions. The small packet size is justified by the relative slow wave speeds and the need of a low BER.

### 5.2 Wireless Network Description

The wireless network carries peer-to-peer single-hop transmissions where packets are stored-and-forwarded from node to node during each transmission. Each node can either act as an end system or a relay and is uniquely identified by its node id. The consequent sections identify important wave farm components and how these affect wireless communication process.

### 5.3 Payload

The payload exerted on the network can be determined from the wave state information generated at each WEC and the handshaking need between the wave farm's main controller and the offshore base station to run *health* and GRID load checks.

The wave speed, period, height and phase angle obtained at each WEC is mainly dependent on its period. Waves off the coast of Oregon have dominant wave periods between six and twenty seconds that results in wave velocities between 9.3 and 31.2 m/s [40]. A wave travelling at 31.2 m/s will traverse the 100 m distance between WEC nodes in 3.2 seconds. For predictive control purposes however, wave sampling must occur at every 0.1 sec over 3-second intervals [40]. Table 1.2 shows the average wave state collected by a *wave rider* off the coast of Oregon [40].

**Table 1.2 Wave state description**

Wave Information	Measurement	Number of bits
Significant Wave Height	10.5 ft	5
Swell Height	6.2 ft	4
Swell Period	10.5 sec	5
Swell Direction	WSW	5
Wind Wave Height	8.5 ft	5
Wind Wave Period	9.9 sec	5
Wind Wave Direction	W	4
Wave Steepness	Average	5
Average Wave Period	7.6 sec	5
Average Wave Speed	65 ft/sec	7



In addition to wave state, other processes, which add to the overall payload, are wave farm *health* reports and GRID load requests (every 20 mins). When sampling waves at every 0.1 sec on 3-second intervals as shown in Table 1.3, the total load is roughly 2000 bits per second (bps). Also listed in Table 1.4 is the packet header used for our simulations. In the next section we discuss data flows among WECs in the wave farm.

**Table 1.3 Payload**

Process	Contribution
Wave State	1920 bps ( $f_s = 0.1s$ , 3 sec interval)
Wave Farm Health Check	1 bps (600 bits/20 min intervals)
GRID load requests	1bps (200 bits/20 min intervals)

**Table 1.4 Packet Structure**

Field	Number of bits
Address	5
Source	5
Data	32
Checksum	4
Start delimiter	1
End delimiter	1
Packet Type	5
Relay Flag	1
UsingRelay	3
TimeSlotNo	3
Relay Address	5
Broadcast ID	5
Total Packet Size	64

## 5.4 Wave State Information Flow

Wave state information flow begins when the waves are first detected by the wave riders positioned on the outskirts of the network as shown in Figure 5.1. The wave riders then transmit this information to the nearest *downstream* WECs or *first row* as shown in the figure. Similarly subsequent transmissions then follow to subsequent rows. From the figure it can be seen that *rows* are formed depending on incoming wave direction. Virtual rows play an important role because they help identify the downstream WECs in the network where a new state is to be transmitted next.

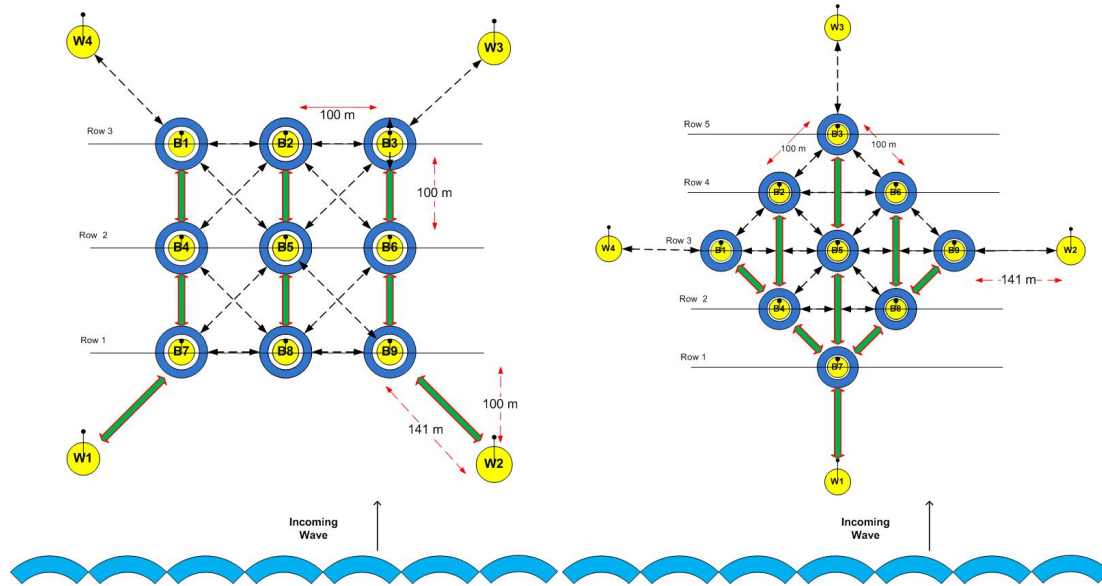


Figure: 5.1 On the left a virtual set of rows is implied when an incoming wave comes at zero degrees of incidence with respect to the network's  $x$ - $y$  coordinate system. The network shown on the right faces an incoming wave at 45 degrees.

## 5.5 Transmission Sequence and Channel Partitioning

The protocol requires equal channel partitioning and sequential transmissions among all the nodes in the network as shown in Figure 5.1 and Fig 5.2. Order is an important aspect in order to keep consistency between waves and the predictive control algorithm for each WEC. The order is controlled and coordinated by the wave farm controller (i.e. B9 in Figure 5.1) by allocating nodes into time frames and each frame into time slots. A node is only allowed to transmit during its allocated time slot as shown in Figure 5.2. The process is repeated like a round-robin (RR) tournament after the last node in the network finishes transmitting. Figure 5.2 shows how TDM helps maintain order among all the nodes.

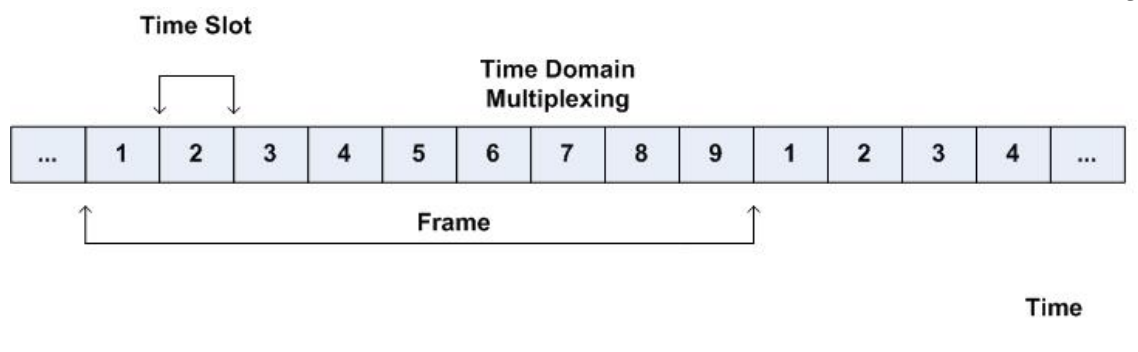


Figure: 5.2 Time allocations per frame and time slot.

## 5.6 Transmit-Relay Process

When a source transmits to a destination node, a relaying slot and two acknowledgement slots follow the initial packet. This idea is shown in Figure 5.3, where we have used the term *sub-time slot* (STS) to distinguish this time allowed within each node transmission turn depicted in Figure 5.2. Included in the packet header is a flag indicating the protocol is using a relay, followed by a field for the relay's address and a *sub-time slot* number. If the relay receives a correct copy of the transmitted packet, it simply forwards it to the destination during its time slot. In addition, the relays flags the packet header indicating the copy being sent is coming from the relay and not from the destination. By doing it in this way, it will allow the destination to know what time slot to use to send back the acknowledgment.

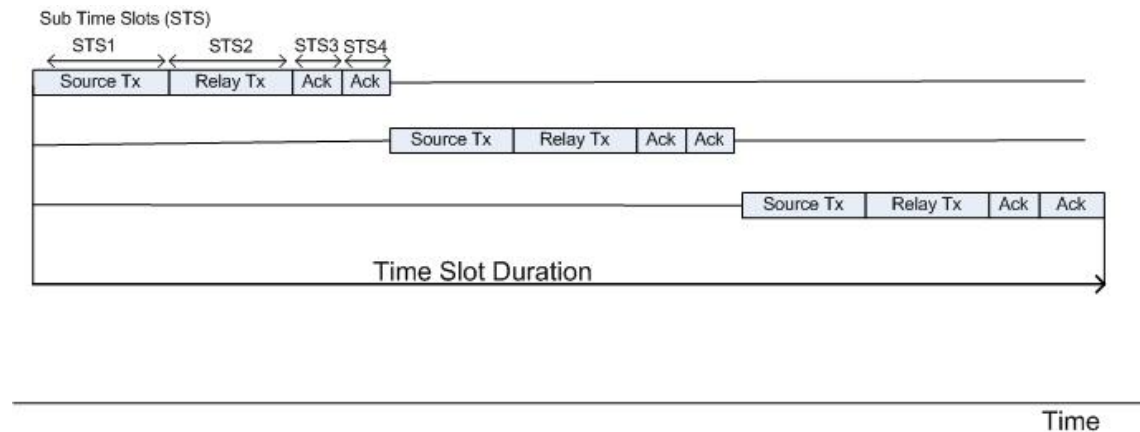


Figure: 5.3 Time slot allocation during a transmission process.

When the source fails to receive a positive ACK from the destination after a certain time deadline, if the relay has a correct copy it then precedes with a retransmission. In a case where both the relay and destination fail to receive the transmitted packets but there is still time within the time slot duration for a retransmission, the source restarts the transmitting process again. Without loss of generality, we assume no ACK is corrupted and lost along the handshaking process. The incoming wave shown in Figure 5.4 is a possible scenario where the relaying protocol can be used.

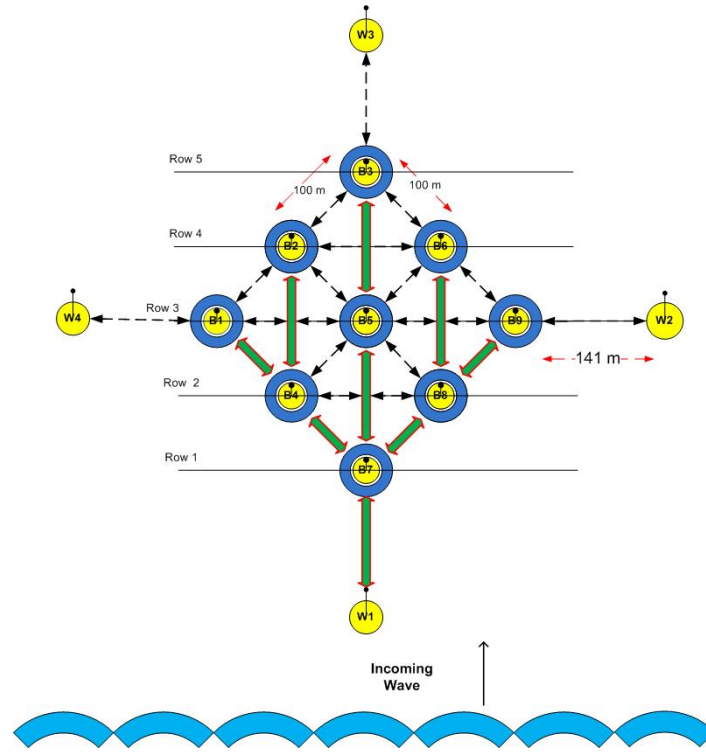


Figure: 5.4 Wave state flow to downstream WECs. Wave rider 1 initiates the process. The different transmissions and retransmissions take place during one time slot. Each slot is then broken up into *sub-time slots*.

## 5.7 Time Slot Duration

Time slot duration depends on how fast new information needs to be transmitted. From section 5.3, the sampling frequency  $f_s$  was equal to 0.1 sec., therefore the time slot duration is also equal to 0.1 sec.

## 5.8 Communication Types

### 5.8.1 Network Health Status

It is important to be able to periodically check the working conditions of each WEC as well as the communication nodes to provide quick maintenance if necessary and maximize electricity throughput. Our work uses the term *Poking* to identify working and non-working communication nodes. This is a similar procedure used by standards [24] except our work uses a simplified version. In particular, each node sends a

CHECKSTATUS request (i.e. status request) to each of its neighbors during its designated time slot. The querying node then records any acknowledgements (ACK) received by its fully functional neighbors. If a neighbor fails to acknowledge after several attempts, its ID is tagged and reported to the wave farm controller. Each node repeats this process at every twenty-minute interval. Furthermore, nodes involved during this process cannot process other tasks such as wave state processing. While the querying node waits for its neighbor's *communication health status report*, the requesting node also queries the local WEC controller about the energy converter status and records it. The *Poking* process is also illustrated in Figure 5.5.

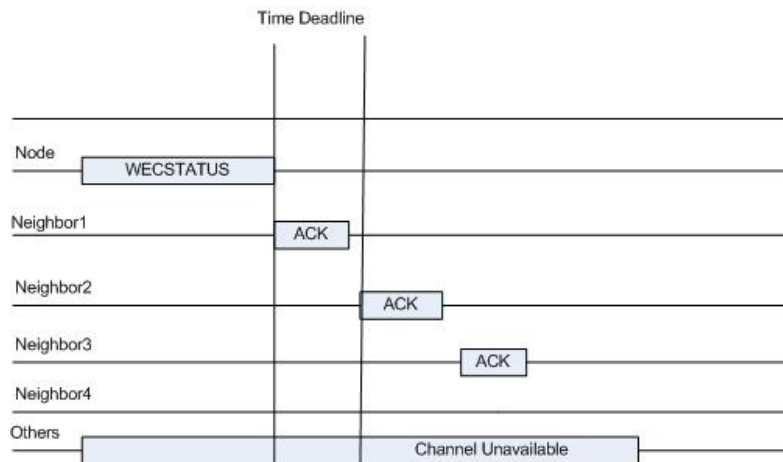


Figure: 5.5 The *poking* process. Neighbors 1,2,3 positively respond while neighbor 4 does not. Neighbor 4 is identified as a malfunctioning device if it fails to positively ACK after several attempts.

### 5.8.2 GRID Load Requests

The wave farm controller initiates the grid load requests at a different twenty-minute interval from the *poking* process. The controller sends a GRIDLOAD packet to an off shore base station as shown in Figure 5.6. The WECs working conditions is also reported during this handshaking process.

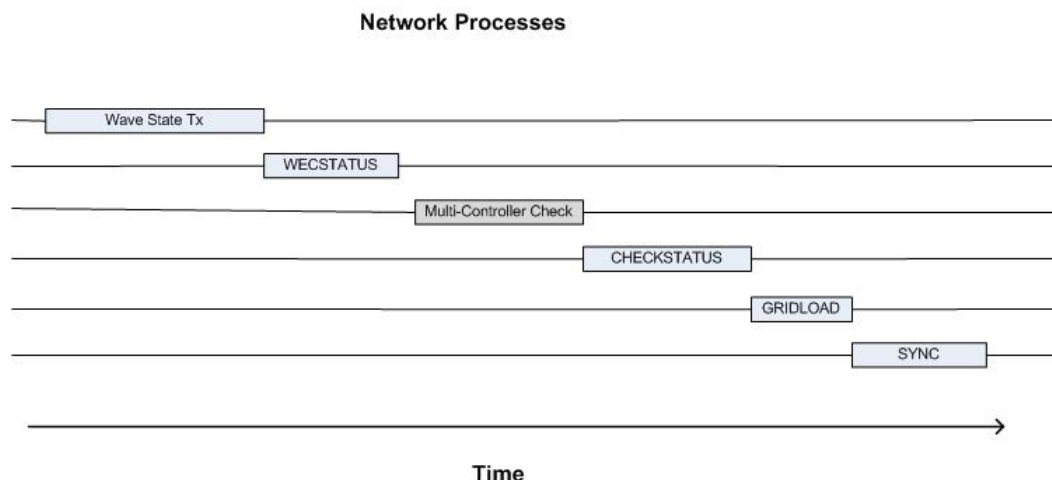


Figure: 5.6 Illustrates how the processes are executed with respect to time.

Finally the wave farm controller sends a SYNC packet after each GRIDLOAD request to ensure clock synchronization among all nodes in the network.

### 5.8.3 Wave Farm Expandability

So far we have introduced a network consisting of nine WECs, however the concept could be applied to multiple *network instances*. In other words, adding more WECs will not alter our design. An example is shown in Figure 5.7, where another *network instance* has been added. When a network consists of more than one *network instance*, the base station can either be given more transmitting power to reach the far end nodes and enforce TDM or a sub-network can be configured to work in synch with the *parent* networks as in Figure 5.7. In either case, both solutions are feasible and practical without adding too much complexity to the over all system.



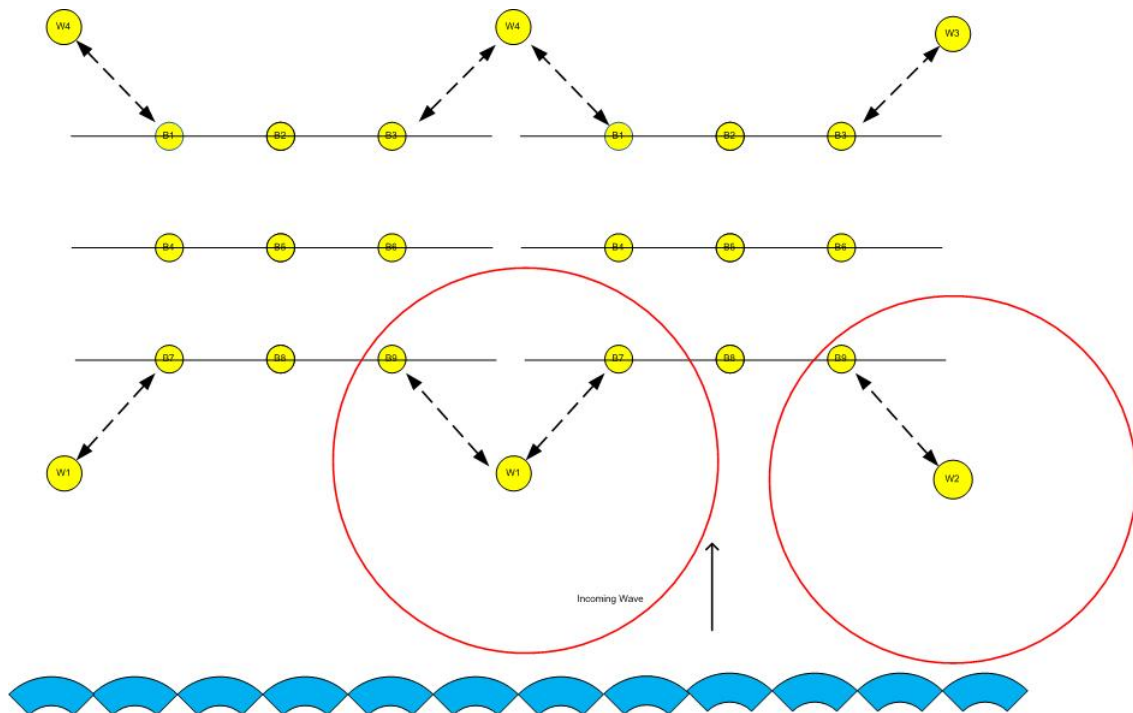


Figure: 5.7 Multiple transmissions within more than one *network instance*.

## 5.9 Packet header

The packet header contains the source address, destination address, relay address, data, and broadcast ID as shown in Figure 5.8. The broadcast ID is used to prevent duplicated messages during broadcasts.

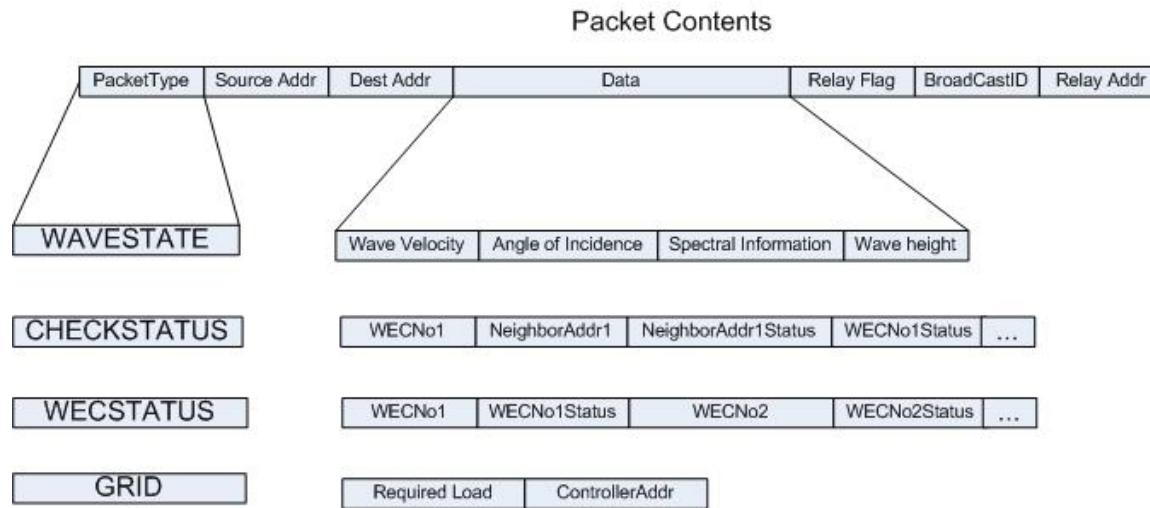


Figure: 5.8 Packet organizations.

### 5.10 Relaying Protocol Performance

Performance is evaluated based on the BER and the average packet delivery delay. The simulations presented in this work are carried out via Matlab and C++.

## 6 SIMULATION RESULTS

### 6.1 Parameters

Many Monte Carlo runs are conducted for the relay networks presented in this work. The simulations have been parameterized to have a spectral efficiency of  $R = 1$  bit/s/Hz. Thus for cooperative transmissions, the rate has been increased to maintain the same spectral efficiency as with non-cooperative networks. BPSK modulation is used for direct transmissions while QPSK for cooperative transmissions. The relay networks simulated in this work have normalized distances between each node as shown in Figure 6.1. The network shown in the figure assumes to be statistically symmetric with channel coefficients  $h_{i,j} = h_{j,i}$  and  $\sigma = 1$ , where  $(i,j)$  are the CSI indices with respect source, relay and destination respectively. The amplification factor for the AAF protocol is set to  $\beta = 1$ , as described in earlier chapters. Performance is evaluated based on the BER and the average packet delivery delay.

### 6.2 Symmetrical Relay Network Used

The symmetrical relay network is shown in Figure 6.1 is used to analyze relay protocol performances in combination with the signal-combining techniques described in earlier sections.

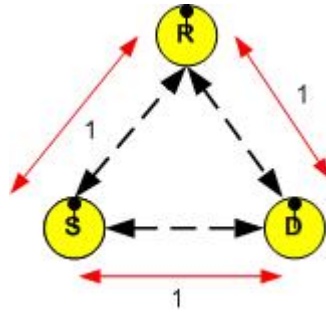


Figure: 6.1 Amplify and Forward (AAF) with No CSI.

### 6.2.1 Combining techniques with AAF - No CSI

The first sets of results we compare are Equal-Ratio Combining and SNR combining. Figure 6.2 and Figure 6.3 show the results obtained after running a MATLAB simulation. The results show that direct transmissions perform better than relayed transmissions at low SNR values. This makes sense in part because the path loss experienced by single transmission is less than the one experienced by the relayed signals. However, if higher transmitting power is used at the source, the relaying scheme outperforms direct transmissions. We list the theoretical performance of 2-antenna array in all figures for comparison purposes only.

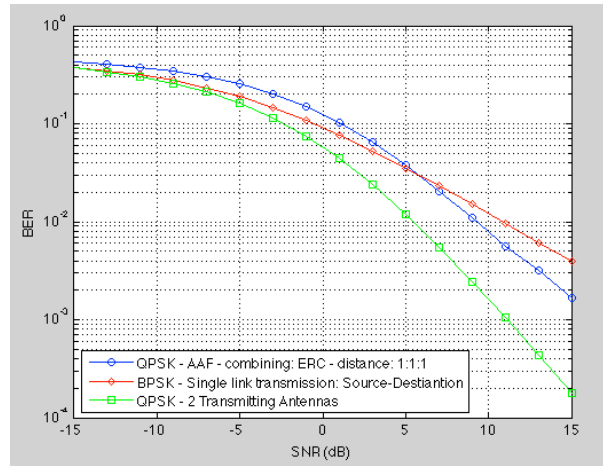


Figure: 6.2 Diversity with ERC vs. Single link transmission.

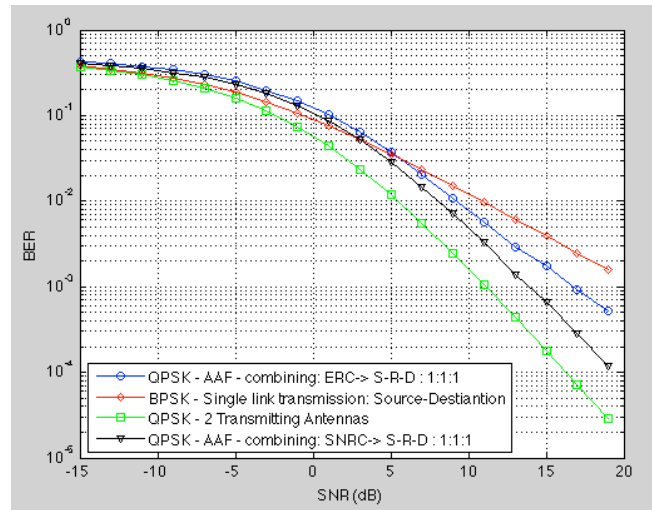


Figure: 6.3 SNR vs. ERC combining using AAF.

### 6.2.2 Combining techniques with DAF - No CSI

The results obtained from simulating DAF are shown in Figure 6.4. Forwarding signals without any knowledge about the CSI and using the SNR combining technique results in similar performance compared to AAF. For ERC, however, it is clear from the figure that its performance degrades. In fact, ERC performs worse than direct transmissions at low SNR values which means that ERC with decode-and-forward should be avoided at all times.

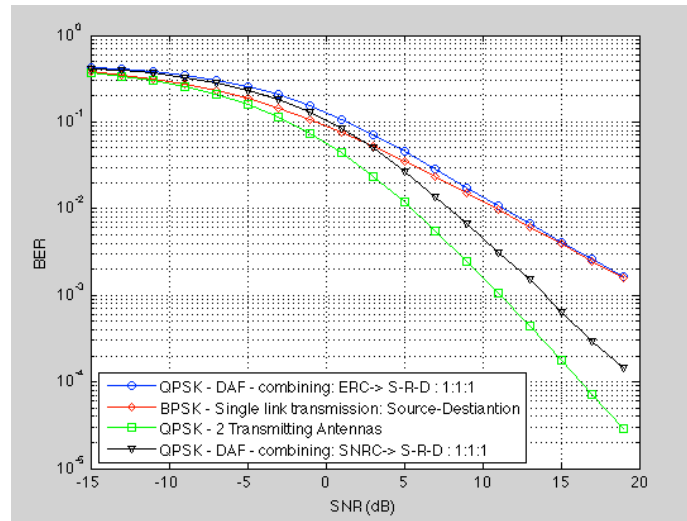


Figure: 6.4 ERC vs. SNRC Comparison.

### 6.2.3 Relaying comparisons between AAF and DAF

The results shown in Figure 6.5 shows that AAF outperforms DAF if equal ratio combining is used at the receiver, whereas DAF outperforms AAF if SNR combining is used instead. The reason for the difference in performance is due to the errors being forwarded to the destination with ERC. The incorrectly detected signals are sent to the destination with the same amount of power as the correct ones, thus, when both signals (from relay and direct transmissions) are decoded at the destination, the receiver has a fifty-fifty chance to correctly decode it. This is different when using AAF; when a deteriorated signal arrives at the relay and it is then amplified before sending it to the destination, the amount of energy (on average) is less than the energy in direct transmissions (assuming the direct link symbol did not suffer from too much fading). Therefore, at the receiver it is likely that the signal sent across the direct link will likely help to correctly decode the symbol after combining them.

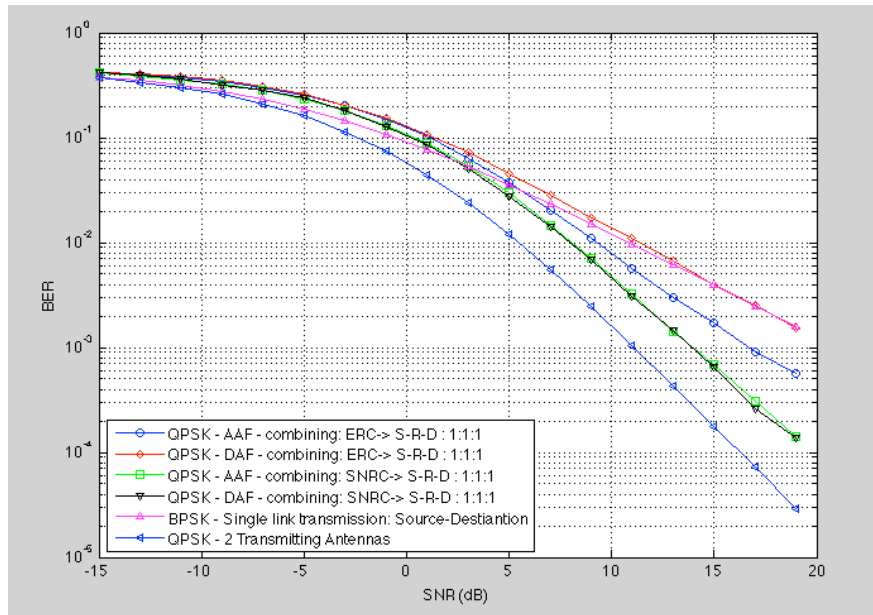


Figure: 6.5 AAF compared to DAF.

#### 6.2.4 AAF vs. DAF Comparison with CSI

The results shown in Figure 6.6 show the comparative results obtained when receivers have complete CSI knowledge. Under these circumstances, MRRC achieves the best BER performance with DAF compared to AAF.

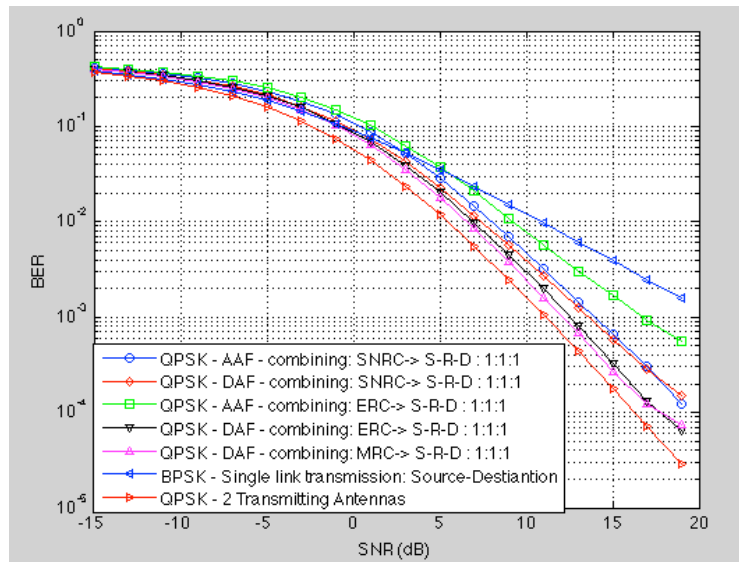


Figure: 6.6. DAF vs. AAF with CSI.

## 7 RELAY POSITIONING

It has been proven that when the relay node is placed close to a source (i.e. at half the distance or closer to the destination node) a clear improvement in BER is achieved [6,48]. This is in part due to the path-loss experienced by the signals along shorter and longer distances compared to direct transmissions. Based on this observation we select the closest relay possible to achieve the best performance.

### 7.1 Relaying Protocol Simulation

#### 7.1.1 Assumptions

We assume each node has sufficient bandwidth to transmit wave state information during a time slot. The channel is assumed to be free from interference caused by other wireless communicating devices transmitting in the 2.4 GHz range or any other standards. The main controller (or access point) directs transmission between nodes and is always active during simulation time. An error correction code is not implemented in this work but rather simulated. Therefore, any packets arriving at the destination containing errors are dropped and a retransmission request is sent to the source. To determine if a packet has been corrupted, a simple checksum is evaluated. We assume block-fading affects the packets, which means that the entire packet undergoes the same fading magnitude due to its short size.

The relaying protocol presented in this work is also simulated using an error correction code. Only error-free symbols are re-transmitted by the relay to the destination and the results are then compared to the relaying protocol without error correction code.

#### 7.1.2 Packet Loss

We assume that each node has enough memory to store the received information packets. Upon processing the received packets by the WEC controller, these are discarded from the receiving queue. The same analogy follows for the transmitting queue. Since no error correction code is implemented in this protocol, any packets failing to pass the checksum at the receiver are dropped and a retransmission process begins.



### 7.1.3 Network Throughput

We define network throughput as the ratio between total number of correctly received bits versus those transmitted.

### 7.1.4 Simulation Parameters

Table 1.5 lists the parameters used for the computer simulations presented in this work.

**Table 1.5 Simulation Parameters**

Parameter	Setting
Distance between each node	100 m
Propagation delay	Distance to the farthest node
Transmission rate	2 Kbps
Packet size	64 bits
Broadcast ID	5 bits
Modulation scheme	TDM, BPSK
Path Loss model	Distance based
Fading channel model	Rayleigh fading
Transmission power	40 dBm
Number of nodes	9
Antenna	Omnidirectional

## 7.2 Special Case Scenarios and Results

In this section we consider some of the most important case scenarios where relaying information becomes crucial for optimal communication performance. The 3 by 3 network using realistic waves is shown in Figure 7.1. Next we will present both BER and throughput for each of the cases presented by running a series of Monte Carlo trials. We emphasize that for the special cases and for simulation purposes only, retransmissions are not implemented. The results are presented below.

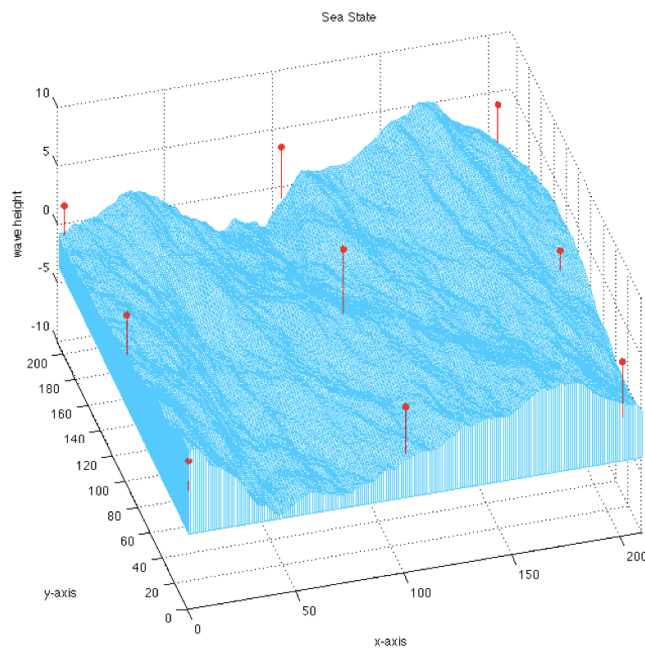


Figure: 7.1 Radio Node Communication Network on a 100 m x 100 m grid.

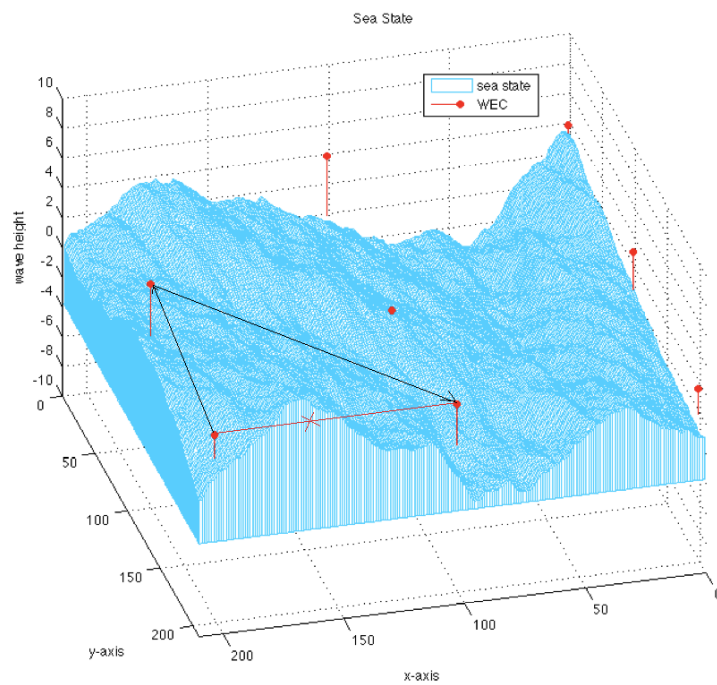


Figure: 7.2 Three-node network.

The results from the network presented in Figure 7.2 are shown in Figure 7.3. The one relay network is especially important because the line of sight between source and destination may be blocked during short instances. The relay can help with retransmissions of any dropped packets by the source.

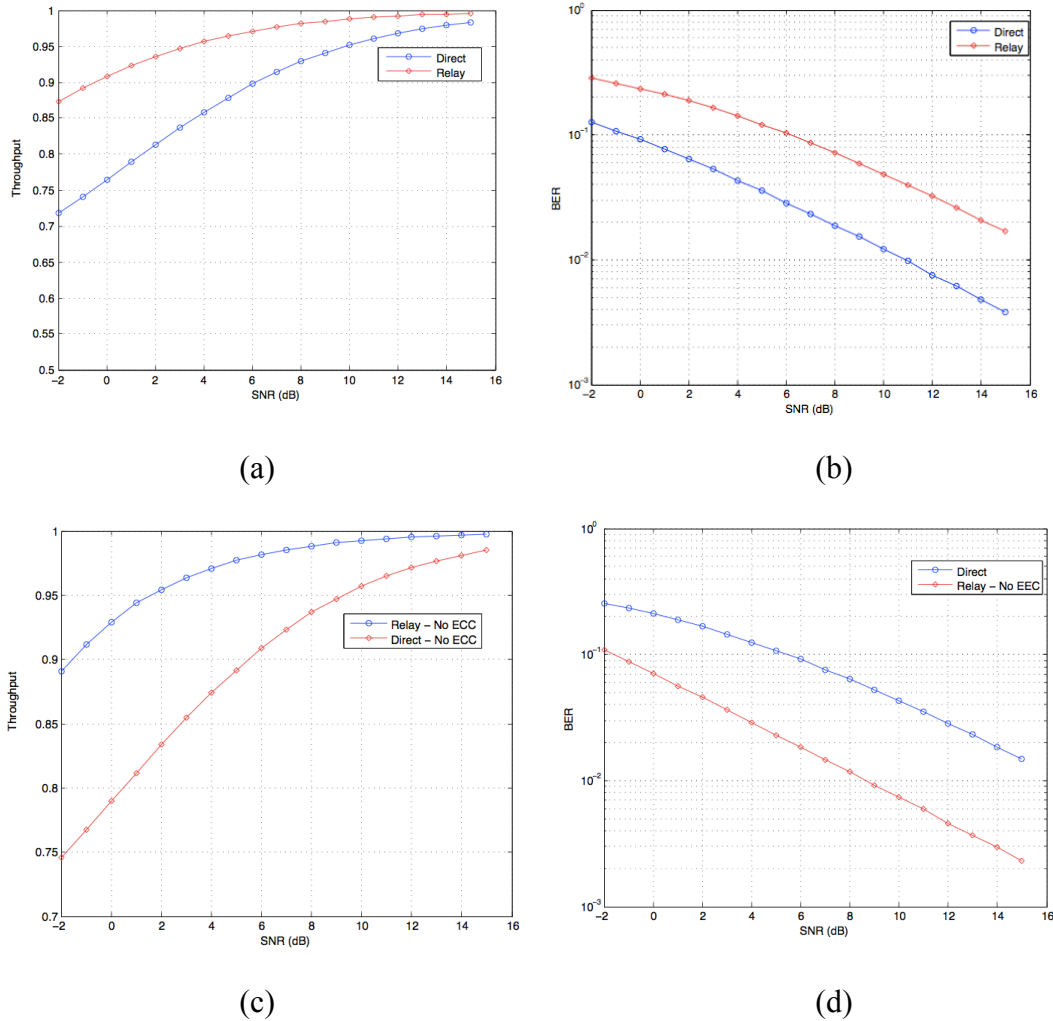


Figure: 7.3 The throughput and BER are shown for a 3-relay network. For (a) & (b) an error correction code algorithm is applied to incoming packets at the relay for comparison purposes only. No error correction is used in (b) & (c).

There may be times where there is more than one relay node available for retransmission as shown in Figure 7.4. Due to the protocol constraints we describe in this work, the source chooses the best relay based on distance and visibility to the destination.

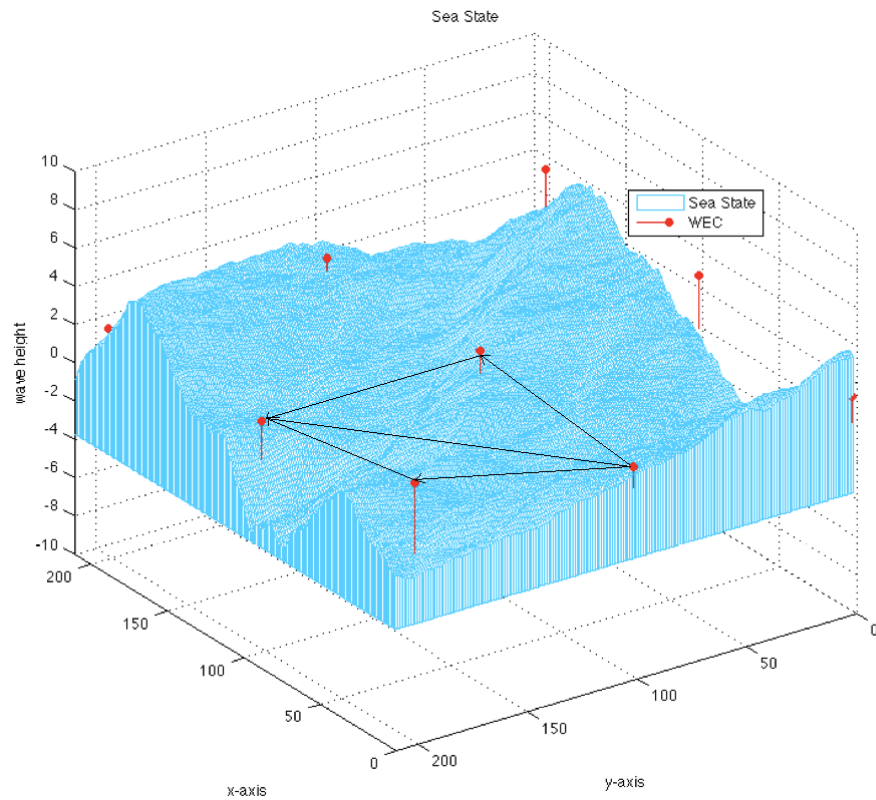


Figure: 7.4 Source with multiple relay options.

There may be cases where the source has no node available to relay information. This case is shown in Figure 7.5, where the center node can only relay on its transmissions to transfer wave state information.

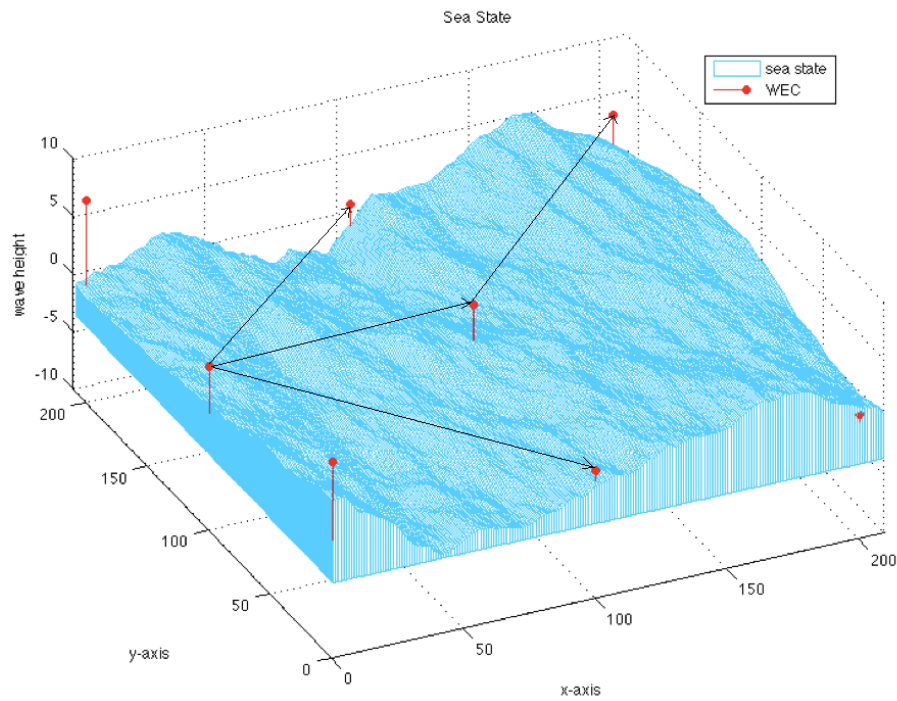
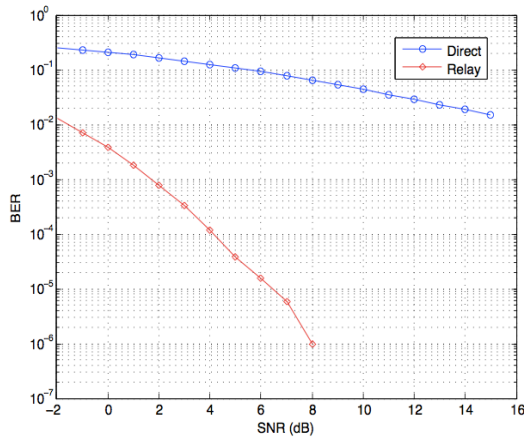
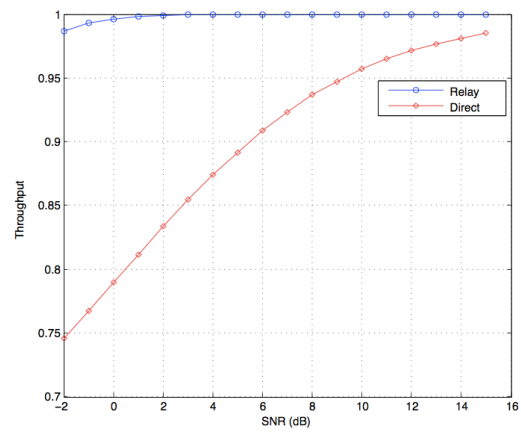


Figure: 7.5 No relay available for source node (center of the plot).

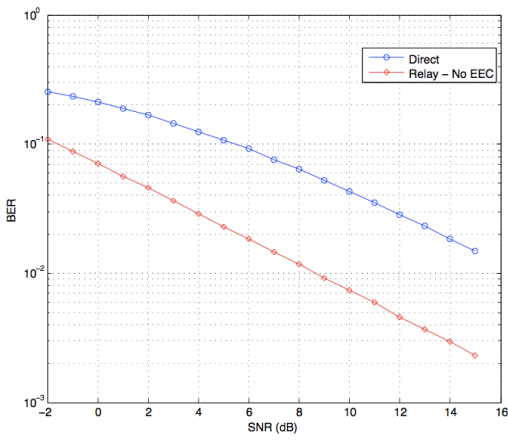
Shown in Figure 7.6 are two relay nodes that can assist the source retransmit information to the destination. Furthermore, although we introduced a one-relay protocol, it could also be expanded to incorporate multiple relays. The simulation results we obtained are shown in Figure 7.7.



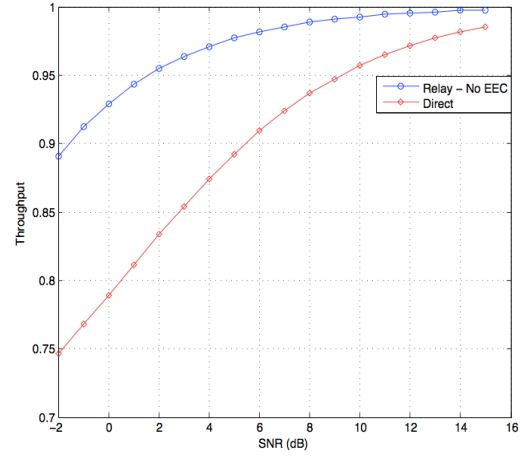
(a)



(b)



(c)



(d)

Figure: 7.6 Scenario where direct transmission is not available but two relays may assist in the transmission process. Plots (a) & (b) show an instance where an error correction code algorithm is applied to incoming packets at the relay. Plots (b) & (c) show the results with no error correction code.

### 7.3 Relaying Protocol Results

The relaying protocol was simulated using one and two retransmissions at the relay. The results clearly show the benefits of using relays in single and double retransmissions as shown in Figure 7.7. In specific, there is a 3dB gain in SNR to achieve the same BER. The protocol is ideal in harsh environment conditions given that each transmission is constrained to a time window with a packet average delay time of approximately 7.2 ms. This is especially beneficial because the wireless network does not cause a bottleneck when nodes stop functioning.

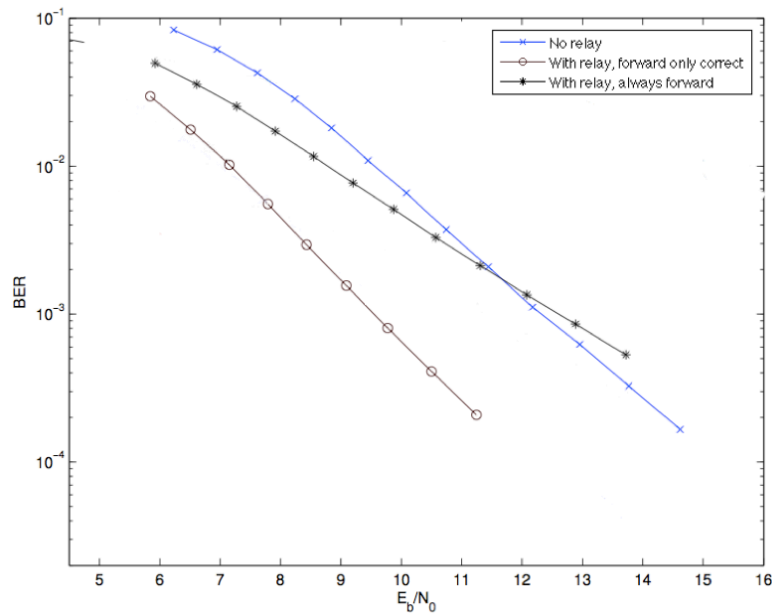


Figure: 7.7 Simulation results using one and two retransmissions.

## 8 Conclusions and Further Work

This thesis has shown the development and validation of a custom, ocean-surface based communication system. The development considered the application of cooperative diversity techniques and a targeted relaying protocol design in order to achieve maximum system reliability in harsh conditions. The system aimed to increase energy conversion in waves includes a method for exchanging information with an on-land base station to provide wave farm maintenance and energy control flow. Although this radio communication design was created specifically for a wave energy farm, it also has other applications in fields of sensor networks or ocean-based wind farms.

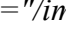
This work showed the importance of using relays in environments where communication links may be obstructed between source and destination. We provided alternatives for improving packet delivery by exploring various relay positioning along the sea surface. The results showed that both BER and throughput can be increased when a relay is positioned with the best line-of-sight and an error correction code is used. Furthermore, a re-transmitting relay protocol was also presented which can further improve reliability by attempting packet retransmissions if necessary. The relay protocol showed a 3 dB SNR improvement over direct transmissions.

This work has shown that a low power communication system is possible even in harsh environmental conditions. In the future, we will continue researching more topics in the predictive control field to fully understand the behavior of ocean waves and their interaction with WECs. We hope to then develop a simulation system that can incorporate the communications, predictive control, and wave simulator and show the improvements in wave energy conversion.



## References

1. Akyildiz, I.F., et al., *A survey on sensor networks*. Communications Magazine, IEEE, 2002. **40**(8): p. 102-114.
2. Alamouti, S.M., *A simple transmit diversity technique for wireless communications*. Selected Areas in Communications, IEEE Journal on, 1998. **16**(8): p. 1451-1458.
3. Alban, E., *Network Coding in Relay Networks*, in *Electrical and Computer Engineering*. 2007, Oregon State University: Corvallis. p. 90.
4. Ali, K. and H. Hassanein. *Underwater Wireless Hybrid Sensor Networks*. in *Computers and Communications, 2008. ISCC 2008. IEEE Symposium on*. 2008.
5. An, J. *Empirical analyses on maritime radio propagation*. in *Vehicular Technology Conference, 2004. VTC 2004-Spring. 2004 IEEE 59th*. 2004.
6. Bader, A. *Single-radio location-based multihop packet relaying*. in *Networking and Services, 2007. ICNS. Third International Conference on*. 2007.
7. Beijar, N *Zone Routing Protocol (ZRP)*. Networking Lab, Helsinki University of Technology.
8. bin Mansor, M.A.A. and J. bin Abdullah. *Evaluating the communication performance of an ad hoc wireless network using Mesh Connectivity Layer (MCL) protocol*. in *Innovative Technologies in Intelligent Systems and Industrial Applications, 2009. CITISIA 2009*. 2009.
9. Boatman, M. *OCS Alternative Energy and Alternate use Programmatic EIS*. 2011 [cited 2011 January 2-May3]; Explores different WEC technologies.]. Available from: <http://ocsenergy.anl.gov/guide/wave/index.cfm>.
10. Brekken, T.K.A., A. von Jouanne, and H. Hai Yue. *Ocean wave energy overview and research at Oregon State University*. in *Power Electronics and Machines in Wind Applications, 2009. PEMWA 2009. IEEE*. 2009.
11. Chakeres, I.D. and E.M. Belding-Royer. *AODV routing protocol implementation design*. in *Distributed Computing Systems Workshops, 2004. Proceedings. 24th International Conference on*. 2004.
12. Charles E. Perkins, P.B., *Highly Dynamic Destination-Sequenced Distance-Vector Routing (DSDV) for Mobile Computers*. 1994: p. 11.
13. Chee-Wei, A. and W. Su. *Signal strength sensitivity and its effects on routing in maritime wireless networks*. in *Local Computer Networks, 2008. LCN 2008. 33rd IEEE Conference on*. 2008.
14. Chia-Sheng, T. and W. Han-Ping. *Study of Routing Protocols for Ocean Surface Communication Networks*. in *Systems, Man and Cybernetics, 2006. SMC '06. IEEE International Conference on*. 2006.
15. Cretel, J.A.M., *Model Predictive Control Applied to a Wave Point Absorber*. 2010, University College Cork: Vilamoura.
16. Energy, U.S.D.o. *Energy Analysis*. 2011 April 06, 2011 [cited May 2010 May 12, 2010]; Wave Energy Distribution in the U.S.]. Available from: <http://www.nrel.gov/analysis/>.
17. Falconer, D.D., F. Adachi, and B. Gudmundson, *Time division multiple access methods for wireless personal communications*. Communications Magazine, IEEE, 1995. **33**(1): p. 50-57.
18. Falnes, J., *OCEAN WAVES AND OSCILLATING SYSTEMS*. 2002, New York: Cambridge University Press.
19. Goldsmith, A., *Wireless Communications*. 2005, New York: Cambridge University Press.
20. Haas, Z.J. *A new routing protocol for the reconfigurable wireless networks*. in *Universal*

- Personal Communications Record, 1997. Conference Record., 1997 IEEE 6th International Conference on.* 1997.
21. Hodtani, G.A. *A new achievable rate for a stochastic two relay network with no interference.* in *Signals, Systems and Computers, 2008 42nd Asilomar Conference on.* 2008.
  22. Hristov, H.D., *Fresnel Zones in Wireless Links, Zone Plate Lenses and Antennas.* 2010.
  23. Hunn, N., *Essentials of Short-Range Wireless.* 2010 ed. 2010, New York: Cambridge University Press.
  24. IEEE, *IEEE 802.4.* 2010, ZigBee. Available at: [standards.ieee.org/about/get/](http://standards.ieee.org/about/get/)
  25. Informer, F. *Wind Power.* 2011; News and Information about Wind Energy Technologies]. Available from: <http://www.alternative-energy-news.info/technology/wind-power/>.
  26. James F. Kurose, K.W.R., *Computer Networking.* Third ed. 2005, \_San Francisco: Pearson Addison Wesley.
  27. Jasani, H. and N. Alaraje. *Evaluating the performance of IEEE 802.11 network using RTS/CTS mechanism.* in *Electro/Information Technology, 2007 IEEE International Conference on.* 2007.
  28. Jin-Teong, O. and H. Chun-Feng. *Propagation measurements on an over-water, line-of-sight link in Singapore.* in *Information, Communications and Signal Processing, 1997. ICICS., Proceedings of 1997 International Conference on.* 1997.
  29. John G. Proakis, M.S., *Digital Communications.* Fifth ed. 2008, New York: McGraw Hill.
  30. Karasawa, Y. and T. Shiokawa, *Fade duration statistics of -band multipath fading due to sea surface reflection.* Antennas and Propagation, IEEE Transactions on, 1987. **35**(8): p. 956-961.
  31. Komen G.J., D.M., M. Cavale, Hasselmann K., Janssen, P., *Dynamics and modeling of ocean waves.* 1994: Cambridge University Press.
  32. Laneman, J.N., D.N.C. Tse, and G.W. Wornell, *Cooperative diversity in wireless networks: Efficient protocols and outage behavior.* Information Theory, IEEE Transactions on, 2004. **50**(12): p. 3062-3080.
  33. Le, S. *Semantic web holds promises for ocean observing needs.* in *OCEANS 2008.* 2008.
  34. McCormick, M.E., *Ocean Wave Energy Conversion.* 2007, New York: Dover Publications, Inc.
  35. Mietzner, J., et al., *Multiple-antenna techniques for wireless communications - a comprehensive literature survey.* Communications Surveys & Tutorials, IEEE, 2009. **11**(2): p. 87-105.
  36. Mingxing, J., et al. *OceanSense: A practical wireless sensor network on the surface of the sea.* in *Pervasive Computing and Communications, 2009. PerCom 2009. IEEE International Conference on.* 2009.
  37. Moffatt, C.D. *High-Data-Rate, Line-of-Site Network Radio for Mobile Maritime Communications (Using Harris WetNet&#8482; Technology).* in *OCEANS, 2005. Proceedings of MTS/IEEE.* 2005.
  38. Mondloch, A., *Overwater propagation of millimeter waves.* Antennas and Propagation, IEEE Transactions on, 1969. **17**(1): p. 82-85.
  39. Muetze, A., *Advanced Independent Study Report Electrical and Computer Engineering Department University of Wisconsin,* in *ECE.* 2005, University of Wisconsin: Madison.
  40. NASA. *National Data Buoy Center.* 2011 [cited April 2010 April 2010]; Available from: <http://www.ndbc.noaa.gov/>.

41. Ohmori, S., et al., *Characteristics of sea reflection fading in maritime satellite communications*. Antennas and Propagation, IEEE Transactions on, 1985. **33**(8): p. 838-845.
42. Ohmori, S. and S. Miura, *A fading reduction method for maritime satellite communications*. Antennas and Propagation, IEEE Transactions on, 1983. **31**(1): p. 184-187.
43. Pathmasuntharam, J.S., et al. *High Speed Maritime Ship-to-Ship/Shore Mesh Networks*. in *Telecommunications, 2007. ITST '07. 7th International Conference on ITS*. 2007.
44. Peng-Yong, K., et al. *A Performance Comparison of Routing Protocols for Maritime Wireless Mesh Networks*. in *Wireless Communications and Networking Conference, 2008. WCNC 2008. IEEE*. 2008.
45. Perkins, C.E. and E.M. Royer. *Ad-hoc on-demand distance vector routing*. in *Mobile Computing Systems and Applications, 1999. Proceedings. WMCSA '99. Second IEEE Workshop on*. 1999.
46. Richter Markus, M.M., Oliver Sawodny, Brekken, Ted, *Power Optimization of a Point Absorber Wave Energy Converter by means of Model Predictive Control*. 2011.
47. Simmons, A., *Evaluating Predictive Control of a Point-Absorber Wave Energy Converter Via Knowledge of Ocean Wave State*. 2011, Oregon State University: Corvallis.
48. Siriwongpairat, W.P., et al. *Optimum threshold-selection relaying for decode-and-forward cooperation protocol*. in *Wireless Communications and Networking Conference, 2006. WCNC 2006. IEEE*. 2006.
49. T, L.M.F.P.H.J.G.R.P.F.M., *Experimental and numerical investigation of non-predictive phase-control strategies for a point-absorbing wave energy converter*. 2010.
50. Tapan Kumar, S., et al., *A deterministic least-squares approach to space-time adaptive processing (STAP)*. Antennas and Propagation, IEEE Transactions on, 2001. **49**(1): p. 91-103.
51. Timmins, I.J. and O.Y. Siu, *Marine Communications Channel Modeling Using the Finite-Difference Time Domain Method*. Vehicular Technology, IEEE Transactions on, 2009. **58**(6): p. 2626-2637.
52. Tsertou, A. and D.I. Laurenson, *Revisiting the Hidden Terminal Problem in a CSMA/CA Wireless Network*. Mobile Computing, IEEE Transactions on, 2008. **7**(7): p. 817-831.
53. Unger, S.M. and R.J. Kraszewski. *Propagation measurements in a shallow water environment*. in *OCEANS '94. 'Oceans Engineering for Today's Technology and Tomorrow's Preservation.' Proceedings*. 1994.
54. Vining, J., *Ocean Wave Energy Conversion*, in *Electrical and Computer Engineering*. 2005, University of Wisconsin: Madison. p. 80.
55. Yapicioglu, T. and S. Oktug. *Effect of wave height to connectivity and coverage in sea surface wireless sensor networks*. in *Computer and Information Sciences, 2009. ISCIS 2009. 24th International Symposium on*. 2009.
56. Yoshio Karasawa, T.S., *Characteristics of L-Band Multipath Fading due to Sea Surface Reflection*. 1984. **AP-32**(No. 6): p. 6.
57. Zimmermann, E., P. Herhold, and G. Fettweis. *On the performance of cooperative diversity protocols in practical wireless systems*. in *Vehicular Technology Conference, 2003. VTC 2003-Fall. 2003 IEEE 58th*. 2003.
58. Zongke, J., et al. *OsnWeb: Sensor Web of OceanSense*. in *Wireless Communications Networking and Mobile Computing (WiCOM), 2010 6th International Conference on*. 2010.